Research Square

Preprints are preliminary reports that have not undergone peer review.
They should not be considered conclusive, used to inform clinical practice,
or referenced by the media as validated information.

The IGF-II/S1P1 receptor transactivation axis: a novel neuroprotective mechanism in Parkinson's disease models

Pablo Zamorano-Gonzalez
Universidad de Málaga
Silvia Claros
Universidad de Málaga
Nadia Valverde
Universidad de Málaga
Estrella Lara
Universidad de Málaga
Silvana Yanina Romero-Zerbo
Universidad de Málaga
René Vidal
Universidad Mayor
Luis J. Santín
Universidad de Málaga
Elisa Martín-Montañez
Universidad de Málaga
Belén Gago
Universidad de Málaga
María García-Fernández
igf@uma.es

Universidad de Málaga

Research Article

Keywords: Parkinson's disease, insulin-like growth factor II, sphingosine-1-phosphate, mitochondrial dysfunction, antioxidant, neuroprotection.

Posted Date: July 27th, 2026

DOI: https://doi.org/10.21203/rs.3.rs-10139023/v1

License: This work is licensed under a Creative Commons Attribution 4.0 International License.
Read Full License

Additional Declarations: No competing interests reported.

Abstract

Background

Parkinson's disease (PD) is characterised by progressive dopaminergic neurodegeneration associated with mitochondrial dysfunction, oxidative stress, and α-synuclein accumulation. Although insulin-like growth factor II (IGF-II) has shown neuroprotective effects in experimental models, its underlying mechanisms remain unclear. This study investigated whether IGF-II protection depends on activation of the sphingosine kinase 1 (SphK1)/sphingosine-1-phosphate (S1P)/$S1P_1$ receptor signalling pathway.

Methods

Neuroprotective effects were evaluated in SN4741 dopaminergic neurons exposed to 1-methyl-4-phenylpyridinium (MPP^+) and in a chronic MPTP/probenecid mouse model of PD. Mitochondrial function, cell viability, sphingolipid metabolism, antioxidant responses, protein expression, and behavioural outcomes were assessed.

Results

MPP^+ induced mitochondrial dysfunction, oxidative stress, prohibitin-2 depletion, and neuronal death. IGF-II restored mitochondrial integrity and cell survival, increased SphK activity, normalised intracellular and extracellular S1P levels, preserved $S1P_1$ receptor expression, and selectively upregulated SphK1. Pharmacological inhibition of SphK1 or $S1P_1$ abolished IGF-II-mediated protection, demonstrating the essential role of this pathway. IGF-II also promoted nuclear translocation of nuclear factor erythroid 2-related factor 2 (Nrf2) and restored antioxidant enzyme activities. In vivo, IGF-II prevented cognitive deficits and anxiety-like behaviour, reduced α-synuclein accumulation, and preserved SphK1 expression in the substantia nigra of MPTP-treated mice.

Conclusions

IGF-II exerts neuroprotective effects through activation of the SphK1/S1P/$S1P_1$ signalling axis, linking mitochondrial preservation, antioxidant defence, and regulation of α-synuclein pathology. Targeting this sphingolipid-dependent pathway may represent a promising disease-modifying therapeutic strategy for PD.

Background

Parkinson's disease (PD) is characterised by the progressive loss of dopaminergic neurons in the *substantia nigra pars compacta* and the depletion of striatal dopamine, leading to severe motor/non-

motor and cognitive impairments (1). While the aetiology of PD is multifactorial, mitochondrial dysfunction and oxidative stress remain central to its pathogenesis (2). Recent evidence indicates that mitochondrial ultrastructural collapse and the loss of inner membrane scaffolds are early events that precede neuronal death (3). Experimental models using the neurotoxins 1-methyl-4-phenylpyridinium (MPP^+) and its precursor 1-methyl-4-phenyl-1,2,3,6-tetrahydropyridine (MPTP) are widely used to mimic these pathological features, as they selectively inhibit mitochondrial complex I, triggering a cascade of reactive oxygen species (ROS) production and programmed cell death (4–7). Current drug treatments for PD focus on symptom management and improving the quality of life in patients. Therefore, there is a need to develop new therapeutic strategies to reverse neuronal damage and halt the progression of the disease. As oxidative stress is a major contributor to nigral loss in both sporadic and genetic forms of PD, it is necessary to identify therapeutic targets with antioxidant effects. Regarding this, recent evidence identifies insulin-like growth factor II (IGF-II) as a neuroprotective factor and a potential therapeutic target in ageing (8), glucocorticoids-induced deleterious effects (9, 10) and neurodegenerative and neuropsychiatric diseases, including Alzheimer's (AD) (11, 12), Huntington's (13), schizophrenia (14), and autism (15). These conditions share common pathogenic mechanisms, such as oxidative stress, mitochondrial and endoplasmic reticulum dysfunction, and synaptic dysregulation (8).

IGF-II, initially considered as a fetal growth factor, has recently emerged as a critical neuroprotective agent in the adult central nervous system (16, 17). Previous studies by our group have demonstrated that IGF-II exerts potent anti-apoptotic and antioxidant effects in dopaminergic neurons by interacting with the IGF-II receptor (IGF-II-R), which triggers the nuclear translocation of nuclear factor erythroid 2-related factor 2 (Nrf2), subsequently inducing the expression of Phase II detoxifying enzymes and preserving mitochondrial integrity by maintaining its membrane potential (18–20). However, the precise molecular mechanism by which IGF-II-R activation triggers these downstream protective responses remains to be fully elucidated, suggesting the involvement of intermediate signalling mediators that bridge receptor activation with organelle stability.

Emerging evidence identifies the sphingosine-1-phosphate (S1P) signalling pathway as a promising candidate in this regulatory network, as it has been shown to function as a link between growth factor receptors (21) and mitochondrial homeostasis (21). S1P is a bioactive lipid that acts as a key "rheostat" of cell fate, with the balance between S1P and its precursors determining whether neurons survive or undergo apoptosis (22, 23). Beyond its role as a signalling molecule, S1P has emerged as a critical mitochondrial metabolic cofactor. By binding to the prohibitin 2 (PHB2) scaffold, intramitochondrial S1P maintains the structural integrity of the cristae and prevents the bioenergetic collapse that characterises dopaminergic neurodegeneration (24). The synthesis of S1P is tightly regulated by sphingosine kinases 1 and 2 (SphK1 and SphK2, respectively). Notably, the expression and activity of these enzymes are significantly dysregulated in the brain tissue of Parkinson's disease patients, thereby contributing to reduced S1P levels and neuronal vulnerability (25). Furthermore, growing evidence indicates that disruption of the S1P pathway contributes to α-synuclein accumulation and aggregation in Parkinson's disease (26). S1P primarily exerts its functions through a family of five specific G protein-coupled

receptors ($S1P_{1-5}$-R) (27). This often involves an "inside-out" signalling mechanism, in which the growth factor triggers intracellular production of S1P, which is then released or acts locally to activate S1P receptors and amplify survival signals (28).

Despite the recognised neuroprotective roles of IGF-II and S1P signalling, the molecular mechanisms underlying their functional interaction in dopaminergic neurodegeneration remain poorly understood. Therefore, elucidating the interaction of these molecules may provide novel mechanistic insights and identify potential therapeutic targets for PD. In the present study, it is hypothesised that the neuroprotective effect of IGF-II against MPP^+/MPTP-induced toxicity is mediated by the 'inside-out' transactivation of the SphK1/S1P/$S1P_1$-R signalling axis. Using the dopaminergic cell line SN4741 and a chronic MPTP mouse model, it is demonstrated that this axis is not only essential for Nrf2-mediated antioxidant responses but nigra acts as a primary regulator of mitochondrial PHB2 levels and mitochondrial permeability transition pore (mPTP) stability, thereby preventing the bioenergetic collapse of the dopaminergic neuron. Furthermore, it is shown that pharmacological inhibition of either SphK1 or $S1P_1$-R completely abolishes the protective effects of IGF-II, confirming that this transactivation mechanism is a mandatory requirement for IGF-II-induced neuronal survival, mitigation of α-synuclein accumulation, and motor recovery in PD models.

Methods

Cell culture

The SN4741 mouse embryonic dopaminergic cell line (RRID: CVCL_S466), which expresses phenotypic markers of *substantia nigra* dopaminergic neurons (29), was kindly provided by Prof. Ernest Arenas (Karolinska Institute, Stockholm, Sweden). Cells were cultured in high-glucose Dulbecco's modified Eagle medium (DMEM; Thermo Fisher Scientific, USA) supplemented with 10% fetal bovine serum (FBS) and 1% penicillin/streptomycin. Culture was maintained at 37 ºC in a humidified atmosphere containing 5% CO_2. For experimental procedures, cells were seeded in either 35 mm^2 glass-bottom dishes or 6-well plates and incubated for 24 hours until reaching approximately 80% confluence.

Cell treatments

To induce Parkinsonian-like neurotoxicity, cells were exposed to 400 µM of MPP^+ (CAS No. 36913–39 –0; Sigma-Aldrich, USA). The neuroprotective potential of IGF-II (25 ng/mL; Lilly Laboratories, Spain) was evaluated either alone or in co-treatment with MPP^+. To dissect the underlying signalling pathways, BMS-536924 (BMS, 1 µM; CAS No. 468740-43-4, Tocris Bioscience, UK), a selective tyrosine kinase inhibitor of the insulin-like growth factor I (IGF-I) and insulin receptors (IGF-I-R and I-R, respectively), was utilised. Concentrations for MPP^+, IGF-II, and BMS were selected based on previous viability assays, in which both IGF-II and BMS were confirmed to be non-toxic under control conditions (30, 31). All compounds

were dissolved in 0.1 M phosphate-buffered saline (PBS), except for BMS, which was prepared in DMSO (< 0.001%).

Before treatment, cells were washed with PBS and then incubated for either 3 or 6 hours, as mentioned in results and Fig. 1a, at 37 ºC in a modified Locke's solution (137 mM NaCl, 5 mM $CaCl_2$, 25 mM glucose, 10 mM KCl, 10 mM HEPES, pH 7.4) supplemented with 1% L-glutamine and 1% penicillin/streptomycin. Experimental groups included: Control (CO, untreated cells in base medium), MPP^+, MPP^++ IGF-II, MPP^++ IGF-II + BMS, and IGF-II alone.

To further investigate the role of the S1P pathway in IGF-II-mediated neuroprotection, specific inhibitors were incorporated using the same experimental design. The involvement of the S1P1 receptor was studied using the selective competitive antagonist W123 (10 µM; CAS nº 1345982-24-2, Cayman Chemicals, USA). The specific roles of SphK isoforms 1 and 2 were assessed using the ATP-competitive inhibitor MP-A08 (Cat. No. 5803, Tocris Bioscience, UK). Based on its dose-dependent selectivity (Ki: 27 µM for SphK1 vs 6.9 µM for SphK2) (32), MP-A08 was used at 40 µM to target SphK1 (iSphK1) and at 9 µM for selective SphK2 inhibition (iSphK2). Following the treatment period, cells were harvested or processed immediately, as required by the specific assay. The experimental timeline and treatment groups are summarised in Fig. 1a.

Cell viability assay

Cell viability was assessed by quantifying lactate dehydrogenase (LDH; EC 1.1.1.27) release into the culture medium, a reliable indicator of plasma membrane integrity. LDH activity was measured in the supernatant following pharmacological treatments using a commercial enzymatic kit (LD3842, Randox Laboratories Ltd., Ireland) adapted for an iCubio spectrophotometric autoanalyser (Biomedical Technology, China). Results were expressed as International Units per millilitre (IU/mL).

Mitochondrial permeability transition pore assay

The opening of the mPTP, a key event in mitochondrial dysfunction and the initiation of apoptotic cascades (33), was evaluated using the calcein-AM/cobalt quenching method (34). This essay relies on the passive diffusion of calcein-AM (10 nM; 56496, Sigma-Aldrich, USA) into the cells, where intracellular esterases cleave the acetoxymethyl ester group, releasing the polar fluorescent dye calcein. While calcein accumulates in both the cytosol and mitochondria, the addition of $CoCl_2$ (0.4 mM; 232696, Sigma-Aldrich, USA) selectively quenches the cytosolic fluorescence, leaving only the mitochondrial calcein signal intact unless the mPTP is opened.

For the assay, cells ($1x10^6$ per condition) were detached using Accutase™ (1000449, MP Biomedicals, USA), collected, and centrifuged to remove the reagent. Pellets were subsequently incubated for 15 minutes at 37 ºC in the dark with calcein-AM and $CoCl_2$ diluted in high-glucose DMEM and PBS,

respectively. As a positive control for pore opening, a group of cells was co-incubated with ionomycin (1 µM; sc-3592, Santa Cruz Biotechnology, USA), a calcium ionophore that triggers mPTP activation and the subsequent loss of mitochondrial calcein fluorescence. Following incubation, cells were centrifuged to remove excess staining and quenching reagents, resuspended in DMEM, and immediately analysed using an Accuri™ C6 flow cytometer and BD Accuri™ C6 software (BD Biosciences, USA). Data were expressed as the rate of mPTP opening relative to the Control group, where an increase in the percentage represents a lower mitochondrial calcein fluorescence.

Sphingolipid metabolism assays

To evaluate the "inside-out" signalling axis, S1P levels and the activities of its key metabolic enzymes were determined.

SphK activity assay. Global SphK (EC 2.7.1.91) activity was measured by quantifying ATP consumption using a commercial luminescent kit (K-3500, Echelon Biosciences, USA). Briefly, cell lysates were incubated with the SphK substrate and ATP for 2h at room temperature. Subsequently, an ATP detector was added and incubated for 10 min, protected from light. Luminescence was recorded at 550 nm using a Varioskan Lux™ spectrophotometer (VLBL00D0, Thermo Fisher Scientific, USA). Results were normalised to protein levels and expressed as a percentage of consumed ATP relative to the Control group.

S1PL activity assay. The enzymatic activity of sphingosine-1-phosphate lyase (S1PL; EC 4.1.2.27) was assessed using a fluorogenic substrate (S-200U, Echelon Biosciences, USA) following the method described in Bedia et al. 2009 (35). This substrate releases fluorescent 7-hydroxycoumarin upon cleavage by active S1PL. Cell lysates were prepared in 0.05 M potassium phosphate buffer (pH 7.2). Briefly, 60 µL of lysate were incubated in a black 96-well plate with 20 µL of a mixture containing 500 µM S-200U, 100 µM Na_3VO_4, and 1 mM pyridoxal 5-phosphate (cofactor). After 6h of incubation at 37 ºC, the reaction was stopped with methanol. Fluorescence was measured at 460 nm (excitation at 355 nm). S1PL activity was expressed as relative fluorescence units per gram of protein, normalised to Control levels.

S1P quantification. Intracellular and extracellular S1P levels were determined using a competitive ELISA kit (K-1900, Echelon Biosciences, USA). For this purpose, SN4741 cells were seeded in 10 cm dishes (2.5 × 10^6 cells/dish) and cultured for 48h to ensure sufficient biomass. Following pharmacological treatments, supernatants were collected and stored at -80 ºC. Cells were detached with Accutase™, washed, and re-suspended in PBS supplemented with protease and phosphatase inhibitors. Cell lysis was performed to release the cytoplasmic content. Both media and cell lysates were processed according to the manufacturer’s instructions.

Antioxidant enzymatic activity assays

Following pharmacological treatment, SN4741 cells were harvested and mechanically lysed in ice-cold PBS (0.1 M, pH 7.4) supplemented with a cocktail of protease and phosphatase inhibitors. The cell suspension was homogenised and subsequently centrifuged at 13,000 x g for 15 min at 4°C. The resulting supernatants were collected for immediate enzymatic analysis. Total protein concentration in the lysates was determined using a NanoDrop™ spectrophotometer (Thermo Fisher Scientific, USA). Enzymatic activities were quantified using a Cobas Mira Autoanalyser (ABX Diagnostics, Germany).

NAD(P)H: quinone oxidoreductase 1 (NQO1; EC 1.6.99.2) activity was assessed by monitoring the decrease in NADH absorbance at 340 nm, consistent with a well-established protocol (36). The reaction mixture contained 25 mM Tris-HCl (pH 7.5), 0.01% Tween 20, 0.7 mg/mL bovine serum albumin (BSA; pH 7.4), 40 µM menadione, 5 µM FAD, 200 µM NADH, and the cell extract. Measurements were recorded at 25-second intervals over 10 min, and one activity unit was defined as the oxidation of 1 µmol of NADH to NAD per minute. All results were expressed as international units of activity per gram of protein.

Simultaneously, Glutathione S-transferase (GST; E.C. 2.5.1.18) activity was determined spectrophotometrically at 340 nm by measuring the formation of the conjugate between 1 mM reduced glutathione (GSH) and 1 mM 1-chloro-2,4-dinitrobenzene (CDNB). One activity unit was defined as the amount of enzyme that catalyses the formation of 1 µmol of S-2,4-dinitrophenylglutathione per minute. All results were expressed as international units of activity per gram of protein.

Immunocytochemical staining

Before seeding, sterile glass coverslips were placed at the bottom of 12-well plates and coated with 1 µg/mL poly-D-lysine (P0899, Sigma-Aldrich, USA). Following the experimental treatments, cells were stained with the mitochondrial marker MitoTracker Deep Red FM (MTR; 200 nM; M22426, Invitrogen™, USA) for 30 min at 37°C, subsequently fixed with ice-cold methanol at -20°C for 20 min, and then exposed to specific primary antibodies overnight at 4°C diluted in PBS/3% BSA: anti-SphK2 (1:50; 17096-1-AB, Proteintech Group, USA), anti-PHB2 (1:50; 12295-1-AP, Proteintech Group, USA), anti-$S1P_1$-R (10 µg/mL; SAB4500687, Sigma-Aldrich, USA) and anti-Nrf2 (1:1000; PA5-88084, Thermo Fisher Scientific, USA). Following primary incubation, cells were treated in the dark for 1h at room temperature with an anti-mouse Alexa Fluor 488 secondary antibody (2 drops/mL; Thermo Fisher Scientific, USA) and DAPI (1:1000; D9542, Sigma-Aldrich, USA) for nuclear counterstaining, before being mounted with Fluoromount (Sigma-Aldrich, USA).

Images were captured using a LEICA Stellaris 8 confocal microscope system (Leica Microsystems AG, Germany) equipped with laser lines at 405 nm, 488 nm, and 641 nm, and initial image processing was performed using Leica LAS AF Lite software. Quantitative analysis was conducted in ImageJ, in which nuclear translocation of Nrf2 was determined by calculating the colocalization area between DAPI-stained nuclei and the total cellular Nrf2 signal. Furthermore, PHB2 distribution was quantified by measuring integrated fluorescence intensity (arbitrary units, AU) within mitochondrial compartments defined by the MTR signal.

Animal model and experimental design

All procedures were approved by the Research Ethics Committee of the University of Málaga (CEUMA Nº 99-2024-A) and were conducted in accordance with Spanish Government guidelines (RD53/2013) and the European Union Council Directive (2010/63/EU). Ten-week-old male C57BL/6J mice (Janvier, France) were housed in groups of 3–4 in standard laboratory cages with nesting material and *ad libitum* access to water and food. Mice were maintained under a 12 h light/dark cycle (lights on at 8:00 a.m.) in a temperature-controlled (22 ± 2ºC) and ventilated room.

Mice were randomly assigned to four experimental groups: Control (n = 8), MPTP (n = 12), MPTP + IGF-II (n = 12) and IGF-II (n = 8). To induce chronic Parkinsonian-like neurodegeneration, a combined regimen of MPTP and probenecid (MPTP/p) was utilised. Mice received subcutaneous (s.c.) injections of MPTP (24 mg/kg; M0896, Sigma-Aldrich, USA) and intraperitoneal (i.p.) injections of probenecid (250 mg/kg; P8761-25G, Sigma-Aldrich, USA) twice a week for five consecutive weeks. Probenecid, initially dissolved in 1 M NaOH and immediately buffered with 0.1 M PBS to pH 7.4, was used to decrease MPTP renal elimination and help maintain a high MPTP concentration in the brain.

The neuroprotective treatment consisted of IGF-II (7.5 µg/kg, s.c.) administered twice daily (every 12h). Notably, the IGF-II treatment followed a preventive protocol, starting one week prior to the first MPTP/p administration and continuing throughout the 5-week lesion period. Following the final MPTP/p dose, IGF-II administration was continued for an additional 10 days to maintain stable levels during behavioural testing. Control and MPTP-only groups received equivalent volumes of 0.9% NaCl (saline) following the same temporal schedule. A detailed representation of the experimental workflow, including the sequence of IGF-II and MPTP/p administrations, is provided in Fig. 4a.

Behavioural testing

Behavioural testing was conducted during the light phase of the light/dark cycle. Animals were habituated to the testing room before each session. All behavioural apparatus was thoroughly cleaned with 70% ethanol between trials to eliminate residual olfactory cues.

Rotarod test. Motor coordination and balance were assessed using an accelerating rotarod apparatus. The protocol included a training phase during which mice underwent three trials per day for three consecutive days to familiarise them with the task. The testing phase began at the onset of IGF-II treatment (week 0) and was conducted weekly for seven consecutive weeks, yielding a total of eight assessment time points. Each testing session consisted of three trials, during which the rod accelerated from 4 to 41 rpm over 5 min. Latency to fall was recorded for each trial, and the sum across the three trials was used for statistical analysis. Results from the week 7 test are shown in Figure S1b.

Self-grooming behaviour. Self-grooming behaviour was quantified as an index of repetitive and affective behaviours. Grooming was recorded during the same 6-minute session used for the Y-maze test to avoid additional handling or stress. Grooming was defined as any licking, scratching, or rubbing of the head,

body, or paws. The total duration of grooming behaviour was manually scored and reported as seconds per session and presented in Figure S1c.

Y-maze spontaneous alternation test. Spatial working memory was evaluated using the spontaneous alternation Y-maze test. The apparatus consisted of three identical arms (30 x 5 x 15 cm) positioned at 120° to each other. Mice were placed at the centre of the maze and allowed to explore freely for 6 min. Spontaneous alternation was defined as successive entries into all three arms without repetition, assessed over overlapping triplet sequences. The percentage of spontaneous alternation behaviour (S.A.B.) was calculated as the number of correct alternations divided by the total number of arm entries minus 2, multiplied by 100. Locomotor parameters, including total travelled distance and mean speed, were also quantified to control for potential motor confounds.

Elevated plus maze. Anxiety-like behaviour was assessed using the elevated plus maze (EPM), consisting of two open arms and two closed arms (arm dimensions: 30 x 5 cm) elevated 50 cm above the floor. Mice were placed on the central platform facing an open arm and allowed to explore the maze for 6 min freely. Anxiety-like behaviour was measured as the percentage of time spent in the open arms relative to total exploration time. Locomotor activity, including total travelled distance and mean velocity, was simultaneously recorded to monitor general motor performance and exclude nonspecific locomotor effects.

Tissue collection and sample preparation

Animals were sacrificed by decapitation 24 h after the final behavioural assessment. Brains were rapidly removed, frozen at -80°C, and subsequently microdissected. The *substantia nigra* was isolated from frozen sections using a biopsy punch technique to ensure anatomical precision and minimise cross-contamination between areas.

For protein analysis, the obtained tissue samples (as well as specific cell culture pellets) were lysed using ice-cold RIPA buffer (sc24948, Santa Cruz Biotechnology, USA) supplemented with a cocktail of protease and phosphatase inhibitors. The homogenates were centrifuged at 11500 x g for 10 min at 4°C to remove cellular debris. The resulting supernatants (cytoplasmic fraction) were collected, and protein concentration was determined using a NanoDrop™ spectrophotometer (Thermo Fisher Scientific, USA). Samples were then aliquoted and stored at -80°C until Western blot analysis.

Western blot analysis

Protein expression was analysed in both SN4741 cell lysates and tissue homogenates. Samples were prepared by mixing 15–30 µg of total protein with Laemmli buffer containing β-mercaptoethanol and heating at 95°C for 5 min. Proteins were resolved using 4–15% Mini-PROTEAN® TGX™ Stain-Free™ precast gels (Bio-Rad Laboratories, USA). Prior to transfer, gels were activated by a 5 min ultraviolet exposure using the ChemiDoc™ XRS+ Imaging System (Bio-Rad Laboratories, USA) to allow for total protein visualization and subsequent normalization. Proteins were then transferred to 0.2 µm pore-size nitrocellulose membranes using the Trans-Blot® Turbo™ Transfer System (Bio-Rad Laboratories, USA).

To prevent non-specific binding, membranes were blocked with 5% non-fat dry milk in Tris-buffered saline containing 0.1% Tween-20 (TBS-T) for 1 h at room temperature. Membranes were then incubated overnight at 4°C with specific primary antibodies diluted in 0.5% BSA. To assess the molecular mechanisms *in vitro*, an antibody against SphK1 (1:1000; sc-365401, Santa Cruz Biotechnology, USA) was utilised in cell lysates. For the *in vivo* characterisation, SphK1, tyrosine hydroxylase (TH; 1:50000; T2928, Sigma-Aldrich, USA), and α-synuclein (1:1000; 610786, BD Transduction Laboratories™, USA) were quantified in *substantia nigra* samples. After washing three times with TBS-T, membranes were incubated for 1 h with HRP-conjugated goat anti-rabbit or anti-mouse IgG (1:1500, both; Bio-Rad Laboratories, USA). Protein bands were detected using SuperSignal™ West Pico PLUS chemiluminescent substrate (Thermo Fisher Scientific, USA) and visualised with the ChemiDoc™ XRS+ system (Bio-Rad Laboratories, USA). Densitometric analysis was performed using Image Lab™ Software (Bio-Rad Laboratories, USA). All target protein levels were normalised to the total protein signal obtained from the Stain-Free gel activation to ensure accurate quantification.

For the analysis of protein expression in the *substantia nigra*, a standardised normalisation control (STD) was utilised to account for inter-gel variability. This standard consisted of a protein pool generated from the *substantia nigra* tissue of four untreated standard mice. This pool was loaded in duplicate on each gel, and the densitometric signals of the experimental samples were normalised to the average STD value within the same blot. For in vivo Western blot analyses, tissue samples from 3–4 mice within the same experimental group were randomly pooled before protein extraction. The same pooled samples were consistently used for the analysis of all protein markers to ensure comparability across targets.

Statistical analysis

Data are expressed as the mean ± standard error of the mean (SEM). Statistical analyses were performed using GraphPad Prism (version 11.0.1). Comparisons between the various experimental groups were analysed using an ordinary one-way Analysis of Variance (ANOVA).

For all analyses, a single pooled variance was assumed, and Tukey's multiple comparisons test was applied as a post-hoc analysis to determine significant differences between all pairs of means. In all cases, a p-value of less than 0.05 ($p < 0.05$) was considered statistically significant. Detailed information regarding specific post-hoc results and p-values is provided in the respective figure legends.

Results

IGF-II preserves mitochondrial integrity and cell viability against MPP^+- insult through a SphK1/$S1P_1$-R-dependent mechanism

Based on our previous findings demonstrating that IGF-II effectively counteracts MPP^+-induced neurotoxicity (20), the present study aimed to elucidate the molecular mechanisms and signalling

pathways involved in this protective effect. As previously reported, exposure of SN4741 dopaminergic cells to MPP^+ resulted in a massive release of LDH into the culture medium (234 IU/mL vs 18 IU/mL in control cells, $p < 0.05$; Fig. 1b), reflecting a significant loss of plasma membrane integrity. This death-like damage was closely linked to a notable 2.9-fold increase in mPTP opening (298% vs 100% in control cells, $p < 0.05$; Fig. 1d).

To further investigate the link between IGF-II and mitochondrial membrane stability, PHB2 levels were measured. PHB2 is a crucial mitochondrial chaperone that not only maintains cristae integrity but also acts as a direct scaffold for sphingolipid signalling within the inner mitochondrial membrane, where it interacts with S1P to regulate respiratory complex assembly (37, 38). Following MPP^+ treatment, a concomitant 56% reduction in PHB2 levels was observed (ratio: 7.8 vs 17.9 in control cells, $p < 0.05$; Fig. 1c,e), confirming that the disruption of the S1P-PHB2 interaction is a hallmark of MPP^+-induced mitochondrial damage.

Incubation in the presence of IGF-II avoids the MPP^+-induced alterations, reverting LDH release (45 IU mL; $p < 0.05$ vs MPP^+ treated cells) and mPTP opening (116.1%) at near control levels, while fully restoring PHB2 expression (ratio: 17) (Fig. 1b-e). Notably, although not statistically significant, IGF-II alone reduces spontaneous mPTP opening (74.2%) and increases PHB2 levels (ratio: 23) compared to control cells (Fig. 1c-e).

SphK1/SphK2 are the primary enzymes involved in S1P synthesis and play a critical role in maintaining the sphingolipid rheostat. To assess their involvement in the neuroprotective effect of IGF-II, a pharmacological approach was used and further assessed their expression levels in our experimental models (see below and Fig. 2e,f). The inhibition of SphK1 (via iSphK1) effectively abolished the beneficial effect of IGF-II, triggering a relapse in LDH release (216 IU/mL) and mPTP opening (254%) (Fig. 1b,d). Similarly, blocking $S1P_1$-R with W123 completely reversed the effect of IGF-II on MPP^+-induced LDH release (Fig. 1b). Conversely, inhibition of SphK2 had negligible effects on cell viability (LDH release: 56 IU/mL) and mitochondrial membrane stability (105%) (Fig. 1b,d). Finally, the use of BMS, which inhibits the tyrosine kinase effect of the IGF-I and insulin receptors (Fig. 1e), confirmed that the neuroprotective effect induced by IGF-II is based on the interaction with its specific IGF-II-R (ratio: 15.9 vs 17.9 in control cells, $p < 0.05$), as it was previously demonstrated by our group (20).

IGF-II regulates sphingolipid metabolism and S1P signalling homeostasis to counteract MPP^+-induced damage

To define the metabolic pathway underlying the neuroprotective effects of IGF-II, the enzymatic machinery, intra- and extracellular S1P availability, and cell membrane $S1P_1$-R were analysed.

Exposing the cells to MPP^+ resulted in a nearly 50% reduction in global SphK activity (53%, $p < 0.05$ vs control cells; Fig. 2a) and a 68% decrease in S1PL activity compared to control cells (Fig. 2b).

Interestingly, while MPP^+ did not significantly alter intracellular S1P levels (108%, ns vs control cells; Fig. 2d), it caused a marked drop in extracellular S1P (68%, $p < 0.05$ vs control cells; Fig. 2c). Furthermore, MPP^+ produced a decrease in membrane $S1P_1$-R (Fig. 2g, I). IGF-II treatment reversed MPP^+ damage, not only restoring global SphK activity (71%, $p < 0.05$ vs MPP^+ treated cells), but also significantly increasing S1P bioavailability at both intracellular (156%) and extracellular (101%) sites (Fig. 2a-c).

Since IGF-II binds to IGF-I and insulin receptors, a strategy was adopted to pharmacologically block these receptors using the antagonist BMS to analyse the effects of IGF-II on its specific receptor. Remarkably, the use of this antagonist further enhances S1P accumulation (131% extra; 220% intracellular), suggesting a specific and potent involvement of the IGF-II receptor in S1P bioavailability. Furthermore, IGF-II partially rescued S1PL activity (57.9%), thereby maintaining S1P signalling flux (Fig. 2b-e).

Moreover, it was confirmed that the selective modulation of the SphK1 isoform drives this metabolic shift. Western blot analysis revealed that while MPP^+ downregulated SphK1 expression (77% vs control cells; $p < 0.05$), while IGF-II prevented this significant loss (103%). This IGF-II-induced upregulation remained insensitive to both BMS (104%) and W123 (116%), confirming that SphK1 induction is an upstream event in the IGF-II signalling cascade (Fig. 2e). Conversely, SphK2 expression remained stable across all experimental conditions (Fig. 2f,h).

Lastly, $S1P_1$-R expression was assessed (Fig. 2g,i), a key component of this pathway. MPP^+ treatment significantly reduced $S1P_1$-R immunofluorescence (83% vs control cells, $p < 0.05$). IGF-II successfully restored and slightly enhanced $S1P_1$-R levels (109% vs control cells, $p < 0.05$), an effect maintained in the presence of BMS (107% vs control cells, $p < 0.05$).

Altogether, these results demonstrate that IGF-II acts as a key regulator of the S1P pathway.

Nrf2 antioxidant response and nuclear recruitment are mechanistically linked to the IGF-II/$S1P_1$ signalling axis.

To study the downstream effectors of the IGF-II/$S1P_1$ axis, Nrf2 pathway activation, the most significant regulator of the cellular antioxidant response, was examined. Firstly, the nuclear/cytoplasmic ratio of Nrf2 immunofluorescence was quantified, as a direct measure of its transcriptional activation (Fig. 3a-b). Exposure to MPP^+ significantly hindered Nrf2 nuclear translocation, yielding a ratio of 0.89 vs 1.39 in control cells ($p < 0.05$). IGF-II treatment not only prevented this impairment but also strongly promoted Nrf2 nuclear recruitment, achieving a ratio of 1.56 ($p < 0.05$ vs MPP+-treated cells), exceeding even the levels in control cells. Consistent with our transactivation hypothesis, the neuroprotective recruitment of Nrf2 was completely abolished when the S1P signalling flux was broken, as both W123 (ratio 0.65) and iSphK1 (ratio 0.85) prevented IGF-II from inducing Nrf2 nuclear translocation.

To confirm whether the observed nuclear translocation of Nrf2 translated into functional enzymatic protection, the specific activities of NQO1 and GST, two critical Phase II detoxifying enzymes, were

measured (Fig. 3c-d). The MPP^+ insult caused a significant reduction in antioxidant capacity, lowering NQO1 activity from 65.4 to 44.8 IU/g protein ($p < 0.05$ vs control cells) and GST activity from 422.9 to 226.5 IU/g protein ($p < 0.05$ vs control cells). IGF-II treatment effectively rescued these enzymatic defences, restoring both NQO1 (60.2 IU/g protein) and GST (341.5 IU/g protein; $p < 0.05$ vs MPP^+ treated cells) activities. Similar to the pattern observed with Nrf2 nuclear localisation, this enzymatic recovery was successfully countered by pharmacological blockade of the S1P pathway. Specifically, the presence of W123 or iSphK1 reduced NQO1 levels to 44.1 and 41.6 IU/g protein ($p < 0.05$ vs MPP + IGF-II treated cells), and GST levels to 253.2 and 249.2 IU/g protein ($p < 0.05$ vs MPP + IGF-II treated cells), respectively.

Collectively, these findings demonstrate that IGF-II triggers a robust antioxidant defence system, mechanistically linked to the SphK1/S1P/$S1P_1$-R signalling pathway.

IGF-II mitigates non-motor deficits and molecular pathology by stabilising the S1P-signalling machinery in the MPTP mouse model

To validate the translational relevance of the IGF-II/S1P axis *in vivo*, a chronic MPTP/probenecid mouse model was used, which consistently replicates the dopaminergic loss and motor impairments previously characterised by our group (20) (see additional data for rotarod, self-grooming, and nigral TH validation). In the present study, the focus was on non-motor symptoms and the underlying molecular shifts.

Assessment of spatial working memory via the Y-maze spontaneous alternation test revealed that MPTP-treated mice exhibited a significant reduction in alternation performance (53.3% vs. 68.5% in control mice; $p < 0.05$), an impairment that was completely restored to control levels by IGF-II co-administration (68.6%) (Fig. 4b). Furthermore, the EPM test revealed a profound anxiety-like phenotype in the MPTP group, evidenced by a dramatic decrease in the time spent in open arms (2.14 sec vs 16.3 sec in control mice, $p < 0.05$; Fig. 4c). Notably, IGF-II treatment effectively counteracted this affective-related deficit, increasing the time in open arms to 13.5 sec.

At the molecular level, it was investigated whether these behavioural improvements were associated with reduced α-synuclein levels and/or the restoration of SphK1 expression. To ensure precise quantification and eliminate inter-experimental variability across multiple Western blots, protein expression levels were normalised against a standardised protein pool (STD), derived from the *substantia nigra* of untreated mice. Under this rigorous protocol, MPTP-lesioned mice showed a substantial increase in α-synuclein levels (118% vs 85% in controls; $p < 0.05$, Fig. 4d), reflecting an accumulation of the protein associated with damaged neurons in a neurodegenerative area. IGF-II treatment significantly attenuated this pathological hallmark, reducing the ratio to 82% ($p < 0.05$ vs MPTP). Similarly, MPTP administration led to downregulation of SphK1 (92.2 vs 112.2 in controls; $p < 0.05$), whereas IGF-II not only prevented this loss but also maintained SphK1 expression at control levels (118.7) (Fig. 4e).

Taken together, these results *in vivo* demonstrate that IGF-II alleviates cognitive and anxiety-like symptoms while preventing α-synuclein accumulation by maintaining the SphK1-mediated signalling.

Discussion

The identification of the IGF-II/SphK1/S1P/$S1P_1$-R activation axis represents a significant advance in understanding the mechanisms of neuronal resilience in Parkinson's disease. Our findings demonstrate that the neuroprotective effect of IGF-II does not rely solely on canonical tyrosine kinase signalling pathways, such as PI3K/Akt and MAPK/ERK kinases, but instead coordinates a sophisticated "inside-out" lipid signalling flux that stabilises mitochondrial function and recruits the Nrf2-mediated antioxidant response. This mechanism effectively couples growth factor-induced survival with the sphingolipid rheostat, a critical metabolic balance that dictates neuronal fate following a profound pathological collapse after MPP^+ administration. By integrating mitochondrial stability, transcriptional regulation, and α-synuclein proteinopathy mitigation, a comprehensive framework is provided that positions the IGF-II/SphK1/S1P/$S1P_1$-R axis as a key regulator of dopaminergic neuronal survival.

At the organelle level, the collapse of mitochondrial integrity constitutes the primary event triggering dopaminergic neuronal death (39, 40). The exposure to the neurotoxin MPP^+, as previously reported by other authors (41), caused a massive increase in reactive oxygen species (ROS), which stimulated the opening of the mPTP (42). This was accompanied by a drastic loss of PHB2, ultimately driving cells toward death, as reflected by the marked increase in LDH release. PHB2 has emerged as an essential scaffold in the inner mitochondrial membrane that interacts directly with S1P to facilitate the assembly of respiratory complexes and maintain cristae morphology, preserving the bio-energetic efficiency (43). In fact, mitochondrial S1P has been proven to bind PHB2 and regulate complex IV (COX) assembly, thereby directly influencing oxidative phosphorylation and ATP production (24). The present study shows that IGF-II, by increasing S1P levels, restores PHB2 levels and prevents mPTP-induced damage induced by MPP^+. This mechanism could explain our previous findings showing that IGF-II restores COX activity and preserves mitochondrial membrane potential (42). Moreover, these results are consistent with previous studies, from our group and others, suggesting that intramitochondrial S1P levels are fundamental for maintaining mitochondrial membrane potential, preventing the release of pro-apoptotic factors such as cytochrome c(44, 45) and restoring redox homeostasis (46, 47).

It is particularly noteworthy that IGF-II alone increased basal PHB2 levels, suggesting a preconditioning or "priming" effect that reinforces mitochondrial ultrastructure and may contribute to the increased mitochondrial spare respiratory capacity previously observed by our group (48). By upregulating the PHB2 scaffold, IGF-II likely optimises the mitochondrial docking sites available for S1P signalling, thereby ensuring that the bioenergetic machinery remains robust even under the toxic stress of Complex I inhibition by MPP^+. This observation complements the mechanistic model proposed by Strub and colleagues, who established that S1P must physically bind to PHB2 to regulate COX activity (24). Without the integrity of this S1P-PHB2 platform, the cell is unable to maintain ATP levels required for

basic homeostatic processes (12), leading to cellular damage and death, as evidenced by LDH release in our MPP^+ model. Furthermore, PHB2, as a core component of the prohibitin complex, exerts chaperone-like functions that support TFAM stability and mitochondrial biogenesis (49). Consequently, the increase in PHB2 expression induced by IGF-II could plausibly contribute to enhanced TFAM levels, in agreement with our previous observations (42) with recent evidence linking prohibitin-dependent mitochondrial organisation to the maintenance of mitochondrial gene expression and respiratory adaptation (50, 51). These observations may be particularly relevant for Parkinson's disease, as PHB2 is now recognised as a key component of the PINK1/Parkin mitophagy machinery required for mitochondrial quality control under conditions of Complex I dysfunction and oxidative stress (52, 53).

The requirement of the SphK1 isoform further highlights the specificity of this protection. Although the balance between pro-apoptotic ceramide and pro-survival S1P establishes the cellular rheostat (54), the functions of SphK1 and SphK2 are remarkably divergent (55). Our pharmacological evidence confirms that only SphK1 inhibition, not SphK2, nullifies the IGF-II-mediated rescue. This distinction is crucial since SphK1 is typically associated with translocation to the plasma membrane and outward signalling via S1P transporters like Spns2 (56, 57), whereas SphK2 has been linked to more complex nuclear functions that may be pro-apoptotic in certain contexts or involved in epigenetic regulation (58). Furthermore, the fact that the antagonist BMS did not prevent S1P accumulation but rather appeared to enhance it suggests that IGF-II may act through its specific receptor. Unlike the IGF-I-R, which is a tyrosine kinase, the IGF-II-R could act as both a G-protein coupled receptor and a clearance receptor, and its activation has been connected to the mobilisation of intracellular calcium and the triggering of sphingosine kinases (59). This bypass of the classical insulin receptor cascade could explain why IGF-II presents a more robust neuroprotective profile than IGF-I in various Parkinson's models, allowing for a more targeted survival response that is less susceptible to the insulin resistance often observed in the neurodegenerative brain (60). This interpretation is further reinforced by the complete abolition of IGF-II neuroprotection following pharmacological inhibition of $S1P_1$-R. Such findings are consistent with the literature describing S1P as a key bioactive lipid that promotes neuronal survival through GPCR-mediated mechanisms (61). Activation of $S1P_1$-R has been shown to engage pro-survival cascades such as PI3K/Akt and MAPK, ultimately inhibiting apoptotic signalling and enhancing cellular resilience (62).

A particularly important aspect of our findings is the observation that MPP^+ selectively impairs extracellular, but not intracellular S1P levels. This suggests that this neurotoxin disrupts S1P export, effectively uncoupling intracellular metabolism from receptor-mediated signalling. Such a mechanism would result in a ligand deficiency at the cell surface, preventing $S1P_1$-R activation despite preserved intracellular S1P pools. This interpretation aligns with clinical observations indicating that reduced circulating S1P levels are associated with a more rapid progression and greater disease severity in PD patients (63). IGF-II appears to overcome this blockade by simultaneously enhancing SphK activity and restoring S1P levels, mainly extracellularly, although it also induces an intracellular increase. The increase in extracellular S1P caused by IGF-II is particularly relevant, as it ensures effective receptor transactivation and downstream signalling. Interestingly, the observation that IGF-I-R/I-R inhibition (via

BMS) may even enhance S1P accumulation suggests a highly specific role for IGF-II-R in regulating this pathway. This specificity is consistent with previous studies demonstrating that IGF-II exerts neuroprotective effects independently of canonical IGF-I-R/I-R signalling, instead relying on mechanisms mediated by IGF-II-R (64, 65).

At the enzymatic level, our data demonstrate that IGF-II induces a robust upregulation of SphK1 expression, further supporting its role as a key regulator of the S1P regulatory axis (66, 67). The fact that this upregulation is insensitive to $S1P_1$-R blockade indicates that SphK1 induction occurs upstream of receptor activation, reinforcing the concept of a hierarchical molecular cascade initiated by IGF-II. In contrast, the stability of SphK2 expression throughout all conditions highlights the isoform-specific nature of this regulatory mechanism, reinforcing the role of SphK1 and its translocation in this context.

An additional layer of regulation within the sphingolipid rheostat uncovered in this study is the impairment of S1PL activity following MPP^+ exposure, which IGF-II partially restored. S1PL is the terminal enzyme responsible for the irreversible degradation of S1P into phosphoethanolamine and hexadecenal, thereby controlling the overall flux and turnover of the sphingolipid pathway (68). Its inhibition is generally associated with a negative feedback response to intracellular S1P accumulation; however, in our model, this effect coexists with a pronounced reduction in extracellular S1P levels, suggesting that MPP^+ primarily disrupts S1P trafficking rather than simply altering its stable concentration. This paradox highlights that S1P bioactivity is not solely determined by total levels, but also by its spatial compartmentalisation and dynamic turnover. Importantly, the partial recovery of S1PL activity induced by IGF-II suggests that the neuroprotective effect is not based on a static increase in S1P, but rather on the restoration of a functional metabolic flux that allows continuous synthesis, release, receptor engagement, and degradation of the lipid mediator. This interpretation aligns with previous reports indicating that proper S1P turnover is essential for maintaining signalling precision (69), as excessive S1P accumulation due to impaired degradation can lead to receptor desensitisation and molecular dysregulation (70).

Our current findings reveal significant downregulation of S1P1-R expression in PD-related neurodegenerative conditions. This observation is consistent with growing evidence indicating that the SphK/S1P/S1PR axis is altered during PD-associated dopaminergic degeneration and may represent an important neuroprotective pathway. For instance, previous studies have reported that pathological α-synuclein accumulation directly impairs the membrane localisation and signalling efficiency of S1P1-R (72). In contrast, chronic dysregulation of the sphingolipid pathway in PD has been shown to induce receptor desensitisation and subsequent internalisation, further depleting the available pool of functional surface $S1P_1$-R (71, 72). Remarkably, our data demonstrates that co-treatment with MPP^+ and IGF-II counteracts this deficit, preventing the decrease in $S1P_1$-R expression. This protective effect may be supported by the molecular crosstalk between growth factors and bioactive sphingolipids (73). Mechanistically, IGF-II stimulates SphK1 translocation to the plasma membrane, driving local S1P synthesis and triggering an autocrine 'inside-out' signalling loop that transactivates and stabilises surface $S1P_1$-R (73, 74). In addition, recent evidence indicates that S1P receptor signalling is involved in

IGF-II/M6P receptor trafficking within the endosomal–Golgi network (75), supporting the possibility that IGF-II may contribute to the maintenance of receptor trafficking and signalling under MPP^+-induced stress. However, further studies will be required to determine whether IGF-II directly stabilises S1P1-R at the plasma membrane, prevents its internalisation/degradation, or preserves its functional coupling in this model.

Collectively, these data indicate that IGF-II appears to re-establish a balanced sphingolipid rheostat, ensuring both sufficient ligand availability for $S1P_1$-R transactivation and restoration of the pro-survival signalling flux, while maintaining an adequate degradation capacity to prevent aberrant receptor activation.

Downstream of $S1P_1$-R activation, our results identify Nrf2 as a critical effector of the IGF-II/S1P signalling axis. Nrf2 is widely recognised as the master regulator of cellular antioxidant defences. It is the principal coordinator of the Phase II detoxification response (75) and its dysfunction is a central feature of the chronic oxidative stress observed in the *substantia nigra* of Parkinson's patients (76, 77). Our findings support that MPP^+ inhibits Nrf2 nuclear translocation, consistent with a collapse of endogenous antioxidant defences previously described by our group (20). IGF-II not only restores but enhances Nrf2 activation beyond basal levels, suggesting a potent amplification of the antioxidant response (20). Crucially, this effect is entirely dependent on SphK1/$S1P_1$-R signalling, as pharmacological inhibition of either component eliminates Nrf2 nuclear recruitment and downstream enzymatic activity (NQO1 and GST). This "crosstalk" aligns with recent research indicating that S1P receptors can modulate the PI3K/Akt and MAPK signalling pathways, which are well-known upstream regulators of Nrf2 stability and its release from its inhibitor, Keap1 (78–80). In this context, our research group has previously demonstrated the key role of the S1P/$S1P_1$-R axis in promoting Nrf2 activation and antioxidant enzyme induction, as well as in preserving mitochondrial function and integrity under neurotoxic conditions (46, 47). By regulating the inside-out S1P flux, IGF-II would create a feedback loop that sustains Nrf2 in the nucleus, reinforcing enzymatic defence against ROS induced by mitochondrial dysfunction, suggesting that the IGF-II-mediated restoration of this pathway is a key determinant of neuronal survival *in vivo*.

The functional relevance of Nrf2 activation induced by IGF-II is confirmed by the restoration of NQO1 and GST activities, two key Phase II detoxifying enzymes that play essential roles in neutralising ROS and maintaining cellular redox balance (20). The ability of IGF-II to counteract the deleterious effects of MPP^+ on these enzyme activities via the IGF-II/SphK1/S1P/$S1P_1$-R circuit further reinforces its role as a potent antioxidant agent, highlighting the importance of the S1P pathway in accomplishing this effect.

Robust data from the chronic MPTP mouse model support the translational significance of this mechanism described in cell culture. Beyond the motor recovery previously characterised by our group (20), it is shown that IGF-II effectively mitigates cognitive and affective-related deficits, including impaired spatial working memory in the Y-maze and anxiety-like behaviour in the EPM, which are critical components of the disease that often precede motor alterations and severely affect patients' quality of

life (81). It is known that fingolimod (FTY720), a S1P receptor modulator (82), was reported to improve cognitive impairment in an essential tremor rat model (83) and that S1P has been proven to promote processes such as synaptic plasticity and neurogenesis, both of which are crucial hallmarks of cognitive health (84–86). Thus, the observed complete recovery of these behavioural parameters by IGF-II treatment suggests that modulation of the S1P pathway may have therapeutic potential beyond motor symptomatology. These findings align with Alberini's research, which highlighted the role of IGF-II in memory formation and implantation (87).

At the molecular level, the reduction in the α-synuclein expression following IGF-II treatment is particularly significant. The α-synuclein aggregation is a well-established feature of PD pathology and is strongly associated with neuroinflammation, mitochondrial dysfunction, oxidative stress, and altered protein degradation pathways (88, 89). Importantly, accumulating evidence suggests that α-synuclein pathology may directly disrupt sphingolipid homeostasis through inhibition of SphK1 activity, leading to sphingosine and ceramide accumulation together with a concomitant reduction in S1P levels, and shifting the sphingolipid rheostat toward a pro-death state (90). In proteomic analysis in our previous work, MPP^+ modified the relative abundance of several 26S proteasome subunits, suggesting a disturbance of proteasome-associated proteostasis (48). Given that impaired protein clearance can favour α-synuclein accumulation and aggregation, the reduction in α-synuclein expression induced by IGF-II treatment is consistent with the idea that IGF-II not only preserves dopaminergic neuronal viability but may also attenuate proteinopathic changes associated with disrupted proteostasis. This interpretation is further supported by previous evidence showing that IGF-II reduces intracellular α-synuclein accumulation and protects dopaminergic neurons in experimental PD models (91). Therefore, it may be hypothesised that part of the neuroprotective effects induced by IGF-II may be partially mediated through modulation of the SphK1/S1P/$S1P_1$-R signalling pathway, which has been linked to neuroinflammatory regulation and protein homeostasis in neurodegenerative disorders (67, 92).

The ability of IGF-II to stabilise the S1P machinery *in vivo*, evidenced by the prevention of SphK1 downregulation in the *substantia nigra*, likely underlies this neuroprotective effect. Given SphK1's significant role in regulating S1P availability and receptor activation, its downregulation in MPTP-treated mice likely contributes to the observed neurodegenerative phenotype (44, 66). Meanwhile, the maintenance of SphK1 levels in the *substantia nigra* of IGF-II-treated mice is consistent with recent evidence indicating that IGF-II stimulation induces SphK1 activation and translocation to endosomal membranes (93). By maintaining SphK1 levels and ensuring S1P bioavailability, IGF-II would not only preserve the integrity of dopaminergic neurons, but it would also generate a less permissive cellular environment for the propagation of proteinopathy.

Conclusions

In conclusion, our findings identify the IGF-II/IGF-II-R/SphK1/S1P/$S1P_1$-R axis as a central neuroprotective mechanism, coordinating mitochondrial preservation, antioxidant defence, and metabolic adaptation in our PD models. By acting as a master regulator of the sphingolipid rheostat, IGF-

II promotes a multifaceted neuroprotective response involving sphingolipid-dependent mechanisms. Through selective activation of SphK1 and transactivation of $S1P_1$-R, IGF-II stabilises mitochondrial integrity via the S1P/PHB2 platform, activates the Nrf2 antioxidant response, restores S1P turnover, and mitigates α-synuclein-associated accumulation. These mechanisms may collectively contribute to alleviating motor and cognitive symptoms. Furthermore, the molecular hallmarks of the disease observed in our experimental models highlight the translational importance of targeting the S1P pathway in PD. Altogether, our results support the idea that the IGF-II/IGF-II-R/SphK1/S1P/$S1P_1$-R axis may represent a promising disease-modifying therapeutic target that can simultaneously address mitochondrial dysfunction, oxidative stress, and impaired proteostasis. Future studies should explore IGF-II analogues or mimetics that reproduce these neuroprotective effects while improving their pharmacokinetic properties.

Abbreviations

AD
Alzheimer's disease
ANOVA
Analysis of variance
ATP
Adenosine triphosphate
AU
Arbitrary units
BMS
BMS-536924
BSA
Bovine serum albumin
CDNB
1-chloro-2,4-dinitrobenzene
COX
Cytochrome c oxidase
DAPI
4',6-diamidino-2-phenylindole
DMEM
Dulbecco's modified Eagle medium
DMSO
Dimethyl sulfoxide
ELISA
Enzyme-linked immunosorbent assay
EPM
Elevated plus maze

ERK1/2
Extracellular signal-regulated kinases 1/2
FAD
Flavin adenine dinucleotide
FBS
Foetal bovine serum
FTY720
Fingolimod
GPCR
G protein-coupled receptor
GSH
Reduced glutathione
GST
Glutathione S-transferase
HEPES
4-(2-hydroxyethyl)-1-piperazineethanesulfonic acid
HRP
Horseradish peroxidase
IGF-I
Insulin-like growth factor I
IGF-I-R
Insulin-like growth factor I receptor
IGF-II
Insulin-like growth factor II
IGF-II-R
Insulin-like growth factor II receptor
i.p.
Intraperitoneal
I-R
Insulin receptor
iSphK1
Sphingosine kinase 1 inhibition/inhibitor
iSphK2
Sphingosine kinase 2 inhibition/inhibitor
IU
International units
Keap1
Kelch-like ECH-associated protein 1
LDH
Lactate dehydrogenase

MAPK
Mitogen-activated protein kinase
MPP^+
1-methyl-4-phenylpyridinium
MPTP
1-methyl-4-phenyl-1,2,3,6-tetrahydropyridine
mPTP
Mitochondrial permeability transition pore
MPTP/p
MPTP/probenecid
MTR
MitoTracker Deep Red FM
NaCl
Sodium chloride
NAD
Nicotinamide adenine dinucleotide
NADH
Reduced nicotinamide adenine dinucleotide
NQO1
NAD(P)H: quinone oxidoreductase 1
Nrf2
Nuclear factor erythroid 2-related factor 2
PBS
Phosphate-buffered saline
PD
Parkinson’s disease
PHB2
Prohibitin 2
PI3K
Phosphoinositide 3-kinase
RIPA
Radioimmunoprecipitation assay
ROS
Reactive oxygen species
rpm
Revolutions per minute
s.c.
Subcutaneous
S1P
Sphingosine-1-phosphate

S1PL
Sphingosine-1-phosphate lyase
$S1P_1$-R
Sphingosine-1-phosphate receptor 1
S.A.B.
Spontaneous alternation behavior
SEM
Standard error of the mean
SphK1
Sphingosine kinase 1
SphK2
Sphingosine kinase 2
Spns2
Spinster homolog 2
STD
Standardized normalization control
TBS-T
Tris-buffered saline + Tween-20
TFAM
Mitochondrial transcription factor A
TH
Tyrosine hydroxylase

Declarations

Competing interests

All authors declare no financial or non-financial competing interests.

Ethics approval

The experimental procedures were carried out in accordance with the ARRIVE guidelines, European Directive 2010/63/EU, and Spanish regulations on animal research, including Royal Decree 53/2013, Royal Decree 1386/2018, and Law 32/2007. The experimental protocols were approved by the Ethics and Research Committee of the University of Málaga (CEUMA 99-2024-A) and by the regional authority, the Regional Ministry of Agriculture, Livestock, Fisheries and Sustainable Development of the Government of Andalusia (No. 14/03/2022/034).

Funding

This study was supported by grants from Junta Andalucia (CTS – 156) GFM as Principal Investigator; the Agencia Estatal de Investigación (PID2020-113806RB-I00/MCIN/AEI/10.13039/501100011033), with GFM and SLJ as Principal Investigator; Agencia Estatal de Investigación (PID2023-149775OB-I00/MCIU/AEI/10.13039/501100011033/FEDER, UE) with MME as Principal Investigator. ZGP was supported by a predoctoral FPI fellowship (PRE2021-09785) from the Ministerio Español de Ciencia e Innovación, associated with the research project PID2020-113806RB-I00, funded by AEI/10.13039/501100011033.

Author Contribution

GFM and MME conceived the idea for the project. GFM, MME, GB, and CS developed or designed the methodology and the in vivo and in vitro models. VN, ZGP, CS, RZSY, LE and GB performed the experiments. SLJ, GB, and MME supervised the study. ZGP, GFM wrote the original draft. GFM, SLJ, and VR reviewed and edited the draft. All authors read, revised, and authorized the manuscript before submission.

Acknowledgement

The authors are grateful to Dr. J. Pavía, retired Professor of Pharmacology, for his valuable comments and assistance during the revision of the manuscript. The authors acknowledge the staff of the Animal Experimentation Centre at the University of Málaga for their valuable assistance during the experiments. We also thank Dr. Ernest Arenas for kindly providing the SN4741 dopaminergic neuronal cell line.This study was supported by grants from Junta Andalucia (CTS -156) GFM as Principal Investigator; the Agencia Estatal de Investigación (PID2020-113806RB-I00/MCIN/AEI/10.13039/501100011033), with GFM and SLJ as Principal Investigator; Agencia Estatal de Investigación (PID2023-149775OB-I00/MCIU/AEI/10.13039/501100011033/FEDER, UE) with MME as Principal Investigator. ZGP was supported by a predoctoral FPI fellowship (PRE2021-09785) from the Ministerio Español de Ciencia e Innovación, associated with the research project PID2020-113806RB-I00, funded by AEI/10.13039/501100011033.

Data Availability

All data are available in the main text or the supplementary materials. All data generated and analyzed during this study are included in this article or available from the corresponding author on reasonable request.

References

1. Morris HR, Spillantini MG, Sue CM, Williams-Gray CH (2024) The pathogenesis of Parkinson's disease. Lancet 403(10423):293–304. 10.1016/S0140-6736(23)01478-2 PubMed PMID: 38245249
2. Kim S, Jung UJ, Kim SR (2024) Role of Oxidative Stress in Blood–Brain Barrier Disruption and Neurodegenerative Diseases. Antioxidants 13(12). 10.3390/ANTIOX13121462
3. Jiang T, Wang J, Li C, Cao G, Wang X, Prohibitins (2022) A Key Link between Mitochondria and Nervous System Diseases. Oxidative Medicine and Cellular Longevity. 10.1155/2022/7494863. PubMed PMID: 35847581 Hindawi Limited
4. Ma Y, Rong Q (2022) Effect of Different MPTP Administration Intervals on Mouse Models of Parkinson's Disease. Contrast Media Mol Imaging 2022. 10.1155/2022/2112146 PubMed PMID: 35299590
5. Santoro M, Fadda P, Klephan KJ, Hull C, Teismann P, Platt B et al (2023) Neurochemical, histological, and behavioral profiling of the acute, sub-acute, and chronic MPTP mouse model of Parkinson's disease. J Neurochem 164(2):121–142. 10.1111/jnc.15699 PubMed PMID: 36184945
6. Mapa MST, Le VQ, Wimalasena K (2018) Characteristics of the mitochondrial and cellular uptake of MPP+, as probed by the fluorescent mimic, 4'I-MPP+. PLoS ONE 13(8). 10.1371/journal.pone.0197946 PubMed PMID: 30138351
7. Blesa J, Przedborski S (2014) Parkinson's disease: Animal models and dopaminergic cell vulnerability. Front Neuroanat. ;8(DEC). 10.3389/fnana.2014.00155 PubMed PMID: 25565980
8. Lewitt MS, Boyd GW (2024) Role of the Insulin-like Growth Factor System in Neurodegenerative Disease. Int J Mol Sci. 10.3390/ijms25084512 PubMed PMID: 38674097
9. Martín-Montañez E, Millon C, Boraldi F, Garcia-Guirado F, Pedraza C, Lara E et al (2017) IGF-II promotes neuroprotection and neuroplasticity recovery in a long-lasting model of oxidative damage induced by glucocorticoids. Redox Biol 13:69–81. 10.1016/j.redox.2017.05.012 PubMed PMID: 28575743
10. Claros S, Cabrera P, Valverde N, Romero-Zerbo SY, López-González MV, Shumilov K et al (2022) Insulin-like growth factor II prevents MPP + and glucocorticoid mitochondrial-oxidative and neuronal damage in dopaminergic neurons. Antioxidants 11(1). 10.3390/antiox11010041
11. Åberg D, Johansson P, Isgaard J, Wallin A, Johansson JO, Andreasson U et al (2015) Increased Cerebrospinal Fluid Level of Insulin-like Growth Factor-II in Male Patients with Alzheimer's Disease. J Alzheimer's Disease 48(3):637–646 doi:10.3233/JAD-150351 PubMed PMID: 26402100
12. Steen E, Terry B, Rivera E, Cannon J, Neely TR, Tavares R et al Impaired insulin and insulin-like growth factor expression and signaling mechanisms in Alzheimer's disease – is this type 3 diabetes? 2005
13. García-Huerta P, Troncoso-Escudero P, Wu D, Thiruvalluvan A, Cisternas-Olmedo M, Henríquez DR et al (2020) Insulin-like growth factor 2 (IGF2) protects against Huntington's disease through the extracellular disposal of protein aggregates. Acta Neuropathol 140(5):737–764. 10.1007/s00401-020-02183-1 PubMed PMID: 32642868
14. Yang YJ, Luo T, Zhao Y, Jiang SZ, Xiong JW, Zhan JQ et al (2020) Altered insulin-like growth factor-2 signaling is associated with psychopathology and cognitive deficits in patients with schizophrenia.

PLoS ONE 15(3). 10.1371/journal.pone.0226688 PubMed PMID: 32191705

15. Steinmetz AB, Stern SA, Kohtz AS, Descalzi G, Alberini CM (2018) Insulin-like growth factor II targets the mTOR pathway to reverse autism-like phenotypes in mice. J Neurosci 38(4):1015–1029 2017 PubMed PMID: 29217683
16. Alberini CM (2023) IGF2 in memory, neurodevelopmental disorders, and neurodegenerative diseases. Trends in Neurosciences. Elsevier Ltd, pp 488–502. 10.1016/j.tins.202303.007 PubMed PMID: 37031050
17. Zhang HY, Jiang YC, Li JR, Yan JN, Wang XJ, Shen JB et al (2023) Neuroprotective effects of insulin-like growth factor-2 in 6-hydroxydopamine-induced cellular and mouse models of Parkinson's disease. Neural Regen Res 18(5):1099–1106. 10.4103/1673-5374.355815
18. Romero-Zerbo SY, Valverde N, Claros S, Zamorano-Gonzalez P, Boraldi F, Lofaro FD et al (2025) New molecular mechanisms to explain the neuroprotective effects of insulin-like growth factor II in a cellular model of Parkinson's disease. J Adv Res 67:349–359. 10.1016/j.jare.2024.01.036 PubMed PMID: 38341032
19. Arcos J, Grunenwald F, Sepulveda D, Jerez C, Urbina V, Huerta T et al (2023) IGF2 prevents dopaminergic neuronal loss and decreases intracellular alpha-synuclein accumulation in Parkinson's disease models. Cell Death Discov 9(1). 10.1038/s41420-023-01734-1 PubMed PMID: 38042807
20. Martín-Montañez E, Valverde N, de Ladrón D, Lara E, Romero-Zerbo YS, Millon C et al (2021) Insulin-like growth factor II prevents oxidative and neuronal damage in cellular and mice models of Parkinson's disease. Redox Biol 46. 10.1016/j.redox.2021.102095 PubMed PMID: 34418603
21. Duan M, Gao P, Chen S, xi, Novák P, Yin K, Zhu X (2022) Sphingosine-1-phosphate in mitochondrial function and metabolic diseases. Obes Rev 23(6). 10.1111/obr.13426
22. Bravo GÁ, Cedeño RR, Casadevall MP, Ramió-Torrentà L (2022) Sphingosine-1-Phosphate (S1P) and S1P Signaling Pathway Modulators, from Current Insights to Future Perspectives. Cells. MDPI. 10.3390/cells11132058 PubMed PMID: 35805142
23. Ueda N (2022) A Rheostat of Ceramide and Sphingosine-1-Phosphate as a Determinant of Oxidative Stress-Mediated Kidney Injury. Int J Mol Sci MDPI. 10.3390/ijms23074010 PubMed PMID: 35409370
24. Strub GM, Paillard M, Liang J, Gomez L, Allegood JC, Hait NC et al (2011) Sphingosine-1-phosphate produced by sphingosine kinase 2 in mitochondria interacts with prohibitin 2 to regulate complex IV assembly and respiration. FASEB J 25(2):600–612. 10.1096/fj.10-167502 PubMed PMID: 20959514
25. Fang J, Wang X, Su X, Li D, Wang F, Wang P et al (2025) Discovery of S1P/SPHK1 dysregulation in Parkinson's disease and its role in pathological α-synuclein-induced neurodegeneration. Innov Life 3(4). 10.59717/j.xinn-life.2025.100164
26. Pyszko JA, Strosznajder JB (2014) The key role of sphingosine kinases in the molecular mechanism of neuronal cell survival and death in an experimental model of Parkinson's disease. Folia Neuropathol 52(3):260–269. 10.5114/fn.2014.45567 PubMed PMID: 25310737
27. Yu L, He L, Gan B, Ti R, Xiao Q, Yang X et al (2022) Structural insights into sphingosine-1-phosphate receptor activation [Internet]. 10.1073/pnas

28. Takabe K, Paugh SW, Milstien S, Spiegel S (2008) Inside-out signaling of sphingosine-1-phosphate: Therapeutic targets. Pharmacol Rev 181–195. 10.1124/pr.107.07113 PubMed PMID: 18552276
29. Son JH, Chun HS, Joh TH, Cho S, Conti B, Lee JW (1998) Neuroprotection and Neuronal Differentiation Studies Using Substantia Nigra Dopaminergic Cells Derived from Transgenic Mouse Embryos
30. Martin-Montañez E, Pavia J, Santin LJ, Boraldi F, Estivill-Torrus G, Aguirre JA et al (2014) Involvement of IGF-II receptors in the antioxidant and neuroprotective effects of IGF-II on adult cortical neuronal cultures. Biochimica et Biophysica Acta (BBA) -. Mol Basis Disease 1842(7):1041–1051. 10.1016/j.bbadis.2014.03.010 PubMed PMID: 24667322
31. Claros S, Cabrera P, Valverde N, Romero-Zerbo SY, López-González MV, Shumilov K et al (2022) Insulin-like growth factor II prevents MPP + and glucocorticoid mitochondrial-oxidative and neuronal damage in dopaminergic neurons. Antioxidants 11(1). 10.3390/antiox11010041
32. Pitman MR, Powell JA, Coolen C, Moretti PAB, Zebol JR, Pham DH et al (2015) Oncotarget 7065 www.impactjournals.com/oncotarget A selective ATP-competitive sphingosine kinase inhibitor demonstrates anti-cancer properties [Internet]. Available from:
33. Baev AY, Vinokurov AY, Potapova EV, Dunaev AV, Angelova PR, Abramov AY (2024) Mitochondrial Permeability Transition, Cell Death and Neurodegeneration. Cells. Multidisciplinary Digital Publishing Institute (MDPI). 10.3390/cells13070648 PubMed PMID: 38607087
34. Petronilli V, Miotto G, Canton M, Brini M, Colonna R, Bernardi P et al (1999) Transient and Long-Lasting Openings of the Mitochondrial Permeability Transition Pore Can Be Monitored Directly in Intact Cells by Changes in Mitochondrial Calcein Fluorescence
35. Bedia C, Camacho L, Casas J, Abad JL, Delgado A, Van Veldhoven PP et al (2009) Synthesis of a fluorogenic analogue of sphingosine-1-phosphate and its use to determine sphingosine-1-phosphate lyase activity. ChemBioChem 10(5):820–822. 10.1002/cbic.200800809 PubMed PMID: 19226506
36. Lind C (1990) ECPHLE. DT-diaphorase: Purification, properties, and function. doi:10.1016/0076-6879(90)86122-C
37. Zhang B, Li W, Cao J, Zhou Y, Yuan X (2024) Prohibitin 2: A key regulator of cell function. Life Sciences. Elsevier Inc.. 10.1016/j.lfs.2023.122371 PubMed PMID: 38142736
38. Duan M, Gao P, Chen S, xi, Novák P, Yin K, Zhu X (2022) Sphingosine-1-phosphate in mitochondrial function and metabolic diseases. Obes Rev 23(6). 10.1111/obr.13426
39. González-Rodríguez P, Zampese E, Stout KA, Guzman JN, Ilijic E, Yang B et al (2021) Disruption of mitochondrial complex I induces progressive parkinsonism. Nature 599(7886):650–656. 10.1038/s41586-021-04059-0 PubMed PMID: 34732887
40. Malpartida AB, Williamson M, Narendra DP, Wade-Martins R, Ryan BJ (2021) Mitochondrial Dysfunction and Mitophagy in Parkinson's Disease: From Mechanism to Therapy. Trends Biochem Sci 46(4):329–343 PubMed PMID: 33323315

41. Cassarino DS, Parks JK, Parker WD, Bennett JP (1999) The parkinsonian neurotoxin MPP+ opens the mitochondrial permeability transition pore and releases cytochrome c in isolated mitochondria via an oxidative mechanism. Biochimica et Biophysica Acta (BBA) - Molecular Basis of Disease. 1453(1):49–62. 10.1016/S0925-4439. (98)00083-0 PubMed PMID: 9989245
42. Martín-Montañez E, Valverde N, de Ladrón D, Lara E, Romero-Zerbo YS, Millon C et al (2021) Insulin-like growth factor II prevents oxidative and neuronal damage in cellular and mice models of Parkinson's disease. Redox Biol 46. 10.1016/ J.REDOX.2021.102095 PubMed PMID: 34418603
43. Signorile A, Sgaramella G, Bellomo F, De Rasmo D, Prohibitins (2019) A critical role in mitochondrial functions and implication in diseases. Cells MDPI. 10.3390/cells8010071
44. Wang W, Zhao Y, Zhu G (2023) The role of sphingosine-1-phosphate in the development and progression of Parkinson's disease. Front Cell Neurosci 17(December). 10.3389/fncel.2023.1288437
45. Ke M, Tang Q, Pan Z, Yin Y, Zhang L, Wen K (2019) Sphingosine-1-phosphate attenuates hypoxia/reoxygenation-induced cardiomyocyte injury via a mitochondrial pathway. Biochem Biophys Res Commun 510(1):142–148 .2019.01.067 PubMed PMID: 30661785
46. Martín-Montañez E, Pavia J, Valverde N, Boraldi F, Lara E, Oliver B et al (2019) The S1P mimetic fingolimod phosphate regulates mitochondrial oxidative stress in neuronal cells. Free Radic Biol Med 137(February):116–130. 10.1016/j.freeradbiomed.2019.04.022 PubMed PMID: 31035004
47. Gil A, Martín-Montañez E, Valverde N, Lara E, Boraldi F, Claros S et al (2020) Neuronal Metabolism and Neuroprotection: Neuroprotective Effect of Fingolimod on Menadione-Induced Mitochondrial Damage. Cells 10(1):34. 10.3390/cells10010034 PubMed PMID: 33383658
48. Romero-Zerbo SY, Valverde N, Claros S, Zamorano-Gonzalez P, Boraldi F, Lofaro FD et al (2025) New molecular mechanisms to explain the neuroprotective effects of insulin-like growth factor II in a cellular model of Parkinson's disease. J Adv Res 67:349–359. 10.1016/j.jare.2024.01.036
49. Champsi S, Hood DA (2025) Role of Prohibitins as Guardians of mitochondrial homeostasis. Mitochondrion 85(March):102075. 10.1016/j.mito.2025.102075 PubMed PMID: 40738239
50. Signorile A, Sgaramella G, Bellomo F, De Rasmo D, Prohibitins (2019) A Critical Role in Mitochondrial Functions and Implication in Diseases. Cells 8(1):71. 10.3390/cells8010071
51. Liu X, Zhang Y, Ni M, Cao H, Signer RAJ, Li D et al (2017) Regulation of mitochondrial biogenesis in erythropoiesis by mTORC1-mediated protein translation. Nat Cell Biol 19(6):626–638. 10.1038/NCB3527 PubMed PMID: 28504707
52. Yan C, Gong L, Chen L, Xu M, Abou-Hamdan H, Tang M et al (2020) PHB2 (prohibitin 2) promotes PINK1-PRKN/Parkin-dependent mitophagy by the PARL-PGAM5-PINK1 axis. Autophagy 16(3):419–434. 10.1080/15548627.2019.1628520 PubMed PMID: 31177901
53. Zhang Y, Yin S, Song R, Lai X, Shen M, Wu J et al (2024) A novel mechanism of PHB2-mediated mitophagy participating in the development of Parkinson's disease. Neural Regen Res 19(8):1828–

1834. 10.4103/1673-5374.389356

54. Ueda N (2022) A Rheostat of Ceramide and Sphingosine-1-Phosphate as a Determinant of Oxidative Stress-Mediated Kidney Injury. Int J Mol Sci MDPI. 10.3390/ijms23074010 PubMed PMID: 35409370
55. Maceyka M, Sankala H, Hait NC, Le Stunff H, Liu H, Toman R et al (2005) SphK1 and SphK2, Sphingosine Kinase Isoenzymes with Opposing Functions in Sphingolipid Metabolism. J Biol Chem 280(44):37118–37129.
10.1074
/jbc.M502207200 PubMed PMID: 16118219
56. Brown RDR, Veerman BEP, Oh J, Tate RJ, Torta F, Cunningham MR et al (2021) A new model for regulation of sphingosine kinase 1 translocation to the plasma membrane in breast cancer cells. J Biol Chem 296.
10.1016/
J.JBC.2021.100674 PubMed PMID: 33865856
57. Siow D, Wattenberg B (2011) The compartmentalization and translocation of the sphingosine kinases: Mechanisms and functions in cell signaling and sphingolipid metabolism. Crit Rev Biochem Mol Biol 365–375. 10.3109/10409238.2011.580097 PubMed PMID: 21864225
58. Diaz Escarcega R, McCullough LD, Tsvetkov AS (2021) The Functional Role of Sphingosine Kinase 2. Frontiers in Molecular Biosciences. Front Media S A. 10.3389/fmolb.2021.683767
59. Wang Y, MacDonald RG, Thinakaran G, Kar S (2017) Insulin-Like Growth Factor-II/Cation-Independent Mannose 6-Phosphate Receptor in Neurodegenerative Diseases. Molecular Neurobiology. Humana Press Inc., pp 2636–2658. 10.1007/s12035-016-9849-7 PubMed PMID: 26993302
60. de la Monte SM (2017) Insulin Resistance and Neurodegeneration: Progress Towards the Development of New Therapeutics for Alzheimer's Disease. Drugs Springer Int Publishing 47–65. 10.1007/s40265-016-0674-0 PubMed PMID: 27988872
61. Binish F, Xiao J (2025) Deciphering the role of sphingosine 1-phosphate in central nervous system myelination and repair. J Neurochemistry John Wiley Sons Inc. 10.1111/jnc.16228 PubMed PMID: 39290063
62. Bryan AM, Del Poeta M (2018) Sphingosine-1-phosphate receptors and innate immunity. Cellular Microbiology. Blackwell Publishing Ltd. 10.1111/cmi.12836 PubMed PMID: 29498184
63. Schwedhelm E, Englisch C, Niemann L, Lezius S, von Lucadou M, Marmann K et al (2021) Sphingosine-1-Phosphate, Motor Severity, and Progression in Parkinson's Disease (MARK-PD). Mov Disord 36(9):2178–2182. 10.1002/mds.28652 PubMed PMID: 34008894
64. Martin-Montañez E, Pavia J, Santin LJ, Boraldi F, Estivill-Torrus G, Aguirre JA et al (2014) Involvement of IGF-II receptors in the antioxidant and neuroprotective effects of IGF-II on adult cortical neuronal cultures. Biochim Biophys Acta 1842(7):1041–1051 .2014.03.010 PubMed PMID: 24667322
65. Romero-Zerbo SY, Valverde N, Claros S, Zamorano-Gonzalez P, Boraldi F, Lofaro FD et al (2025) New molecular mechanisms to explain the neuroprotective effects of insulin-like growth factor II in a

cellular model of Parkinson's disease. J Adv Res 67.
10.1016/J
.JARE.2024.01.036 PubMed PMID: 38341032

66. Motyl J, Strosznajder JB (2018) Sphingosine kinase 1/sphingosine-1-phosphate receptors dependent signalling in neurodegenerative diseases. The promising target for neuroprotection in Parkinson's disease. Pharmacol Rep 70(5):1010–1014. 10.1016/j.pharep.2018.05.002 PubMed PMID: 30138818
67. Pyszko J, Strosznajder JB (2014) Sphingosine kinase 1 and sphingosine-1-phosphate in oxidative stress evoked by 1-methyl-4-phenylpyridinium (MPP+) in human dopaminergic neuronal cells. Mol Neurobiol 50(1):38–48. 10.1007/s12035-013-8622-4 PubMed PMID: 24399507
68. Aguilar A, Saba JD (2012) Truth and consequences of sphingosine-1-phosphate lyase. Advances in Biological Regulation. Elsevier Ltd, pp 17–30. 10.1016/j.advenzreg.2011.09.015 PubMed PMID: 21946005
69. Cartier A, Hla T (2019) Sphingosine 1-phosphate: Lipid signaling in pathology and therapy. Science. American Association for the Advancement of Science. 10.1126/science.aar5551 PubMed PMID: 31624181
70. Gatfield J, Monnier L, Studer R, Bolli MH, Steiner B, Nayler O (2014) Sphingosine-1-phosphate (S1P) displays sustained S1P1 receptor agonism and signaling through S1P lyase-dependent receptor recycling. Cell Signal 26(7):1576–1588 03.029 PubMed PMID: 24704119
71. Zhang L, Okada T, Badawy SMM, Hirai C, Kajimoto T, Nakamura SI (2017) Extracellular α-synuclein induces sphingosine 1-phosphate receptor subtype 1 uncoupled from inhibitory G-protein leaving β-arrestin signal intact. Sci Rep 7. 10.1038/srep44248 PubMed PMID: 28300069
72. Mohamed Badawy SM, Okada T, Kajimoto T, Hirase M, Matovelo SA, Nakamura S et al (2018) Extracellular -synuclein drives sphingosine 1-phosphate receptor subtype 1 out of lipid rafts, leading to impaired inhibitory G-protein signaling. J Biol Chem 293(21):8208–8216. 10.1074/jbc.RA118.001986 PubMed PMID: 29632069
73. Lebman DA, Spiegel S (2008) Cross-talk at the crossroads of sphingosine-1-phosphate, growth factors, and cytokine signaling. J Lipid Res 1388–1394. 10.1194/jlr.R800008-JLR200 PubMed PMID: 18387885
74. El-Shewy HM, Lee MH, Obeid LM, Jaffa AA, Luttrell LM (2007) The insulin-like growth factor type 1 and insulin-like growth factor type 2/mannose-6-phosphate receptors independently regulate ERK1/2 activity in HEK293 cells. J Biol Chem 282(36):26150–26157. 10.1074/jbc.M703276200 PubMed PMID: 17620336
75. Keum YS (2012) Regulation of Nrf2-mediated phase ii detoxification and anti-oxidant genes. Biomolecules Ther 144–151. 10.4062/biomolther.2012.20.2.144
76. Bento-Pereira C, Dinkova-Kostova AT (2021) Activation of transcription factor Nrf2 to counteract mitochondrial dysfunction in Parkinson's disease. Medicinal Research Reviews. John Wiley and Sons Inc, pp 785–802. doi:10.1002/med.21714. PubMed PMID: 32681666

77. ÁJ GY, Dinkova-Kostova NE, AI AT, PG R, NRF2 AT THE CROSSROADS OF PARKINSON'S DISEASE AND AGING: MECHANISTIC INSIGHTS AND TRANSLATIONAL PERSPECTIVES (2026 Mar) Free Radic Biol Med. 10.1016/j.freeradbiomed.2026.01.023 PubMed PMID: 41539374
78. Mercado N, Kizawa Y, Ueda K, Xiong Y, Kimura G, Moses A et al (2014) Activation of transcription factor Nrf2 signalling by the sphingosine kinase inhibitor SKI-II is mediated by the formation of Keap1 dimers. PLoS ONE 9(2). 10.1371/journal.pone.0088168 PubMed PMID: 24505412
79. Safarian F, Khallaghi B, Ahmadiani A, Dargahi L (2015) Activation of S1P1 Receptor Regulates PI3K/Akt/FoxO3a Pathway in Response to Oxidative Stress in PC12 Cells. J Mol Neurosci 56(1):177–187. 10.1007/s12031-014-0478-1 PubMed PMID: 25534920
80. Wang L, Chen Y, Sternberg P, Cai J (2008) Essential roles of the PI3 kinase/Akt pathway in regulating Nrf2-dependent antioxidant functions in the RPE. Invest Ophthalmol Vis Sci 49(4):1671–1678. 10.1167/iovs.07-1099 PubMed PMID: 18385090
81. Liu R, Umbach DM, Tröster AI, Huang X, Chen H (2020) Non-motor symptoms and striatal dopamine transporter binding in early Parkinson's disease. Parkinsonism Relat Disord 72:23–30. 10.1016/j.parkreldis.202002.001 PubMed PMID: 32092703
82. Martín-Montañez E, Pavia J, Valverde N, Boraldi F, Lara E, Oliver B et al (2019) The S1P mimetic fingolimod phosphate regulates mitochondrial oxidative stress in neuronal cells. Free Radic Biol Med 137:116–130 .2019.04.022 PubMed PMID: 31035004
83. Dahmardeh N, Asadi-Shekaari M, Arjmand S, Haghani M, Shabani M (2018) Fingolimod attenuates harmaline-induced passive avoidance memory and motor impairments in a rat model of essential tremor. Ceska Slov Neurologie Neurochirurgie 81(6):691–699. 10.14735/amcsnn2018691
84. Wang W, Zhao Y, Zhu G (2023) The role of sphingosine-1-phosphate in the development and progression of Parkinson's disease. Front Cell Neurosci Front Media SA. 10.3389/fncel.2023.1288437
85. Kanno T, Nishizaki T, Proia RL, Kajimoto T, Jahangeer S, Okada T et al (2010) Regulation of synaptic strength by sphingosine 1-phosphate in the hippocampus. Neuroscience 171(4):973–980. 10.1016/j.neuroscience.2010.10.021 PubMed PMID: 20950672
86. Riganti L, Antonucci F, Gabrielli M, Prada I, Giussani P, Viani P et al (2016) Sphingosine-1-phosphate (S1P) impacts presynaptic functions by regulating synapsin i localization in the presynaptic compartment. J Neurosci 36(16):4624–4634. 10.1523/JNEUROSCI.3588-152016 PubMed PMID: 27098703
87. Alberini CM (2023) IGF2 in memory, neurodevelopmental disorders, and neurodegenerative diseases. Trends in Neurosciences. Elsevier Ltd, pp 488–502. 10.1016/j.tins.202303.007 PubMed PMID: 37031050
88. Wong YC, Luk K, Purtell K, Burke Nanni S, Stoessl AJ, Trudeau LE et al (2019) Neuronal vulnerability in Parkinson disease: Should the focus be on axons and synaptic terminals? Mov Disord 34(10):1406–1422. 10.1002/mds.27823 PubMed PMID: 31483900

89. Lin KJ, Lin KL, Chen S, Der, Liou CW, Chuang YC, Lin HY et al (2019) The Overcrowded Crossroads: Mitochondria, Alpha-Synuclein, and the Endo-Lysosomal System Interaction in Parkinson's Disease. International Journal of Molecular Sciences 2019, Vol 20, Page 5312. ;20(21):5312. doi:10.3390/IJMS20215312 PubMed PMID: 31731450
90. Motyl JA, Strosznajder JB, Wencel A, Strosznajder RP (2021) Recent insights into the interplay of alpha-synuclein and sphingolipid signaling in parkinson's disease. Int J Mol Sci MDPI. 10.3390/ijms22126277 PubMed PMID: 34207975
91. Arcos J, Grunenwald F, Sepulveda D, Jerez C, Urbina V, Huerta T et al (2023) IGF2 prevents dopaminergic neuronal loss and decreases intracellular alpha-synuclein accumulation in Parkinson's disease models. Cell Death Discov 9(1):438. 10.1038/s41420-023-01734-1 PubMed PMID: 38042807
92. van Echten-Deckert G (2023) The role of sphingosine 1-phosphate metabolism in brain health and disease. Pharmacol Ther 244:108381. 10.1016/J .PHARMTHERA.2023.108381 PubMed PMID: 36907249
93. Nishida S, Matovelo SA, Kajimoto T, Nakamura SI, Okada T (2024) Involvement of sphingosine 1-phosphate signaling in insulin-like growth factor-II/mannose 6-phosphate receptor trafficking from endosome to the trans-Golgi network. Commun Biol 7(1). 10.1038/s42003-024-06828-9 PubMed PMID: 39300315

Figures

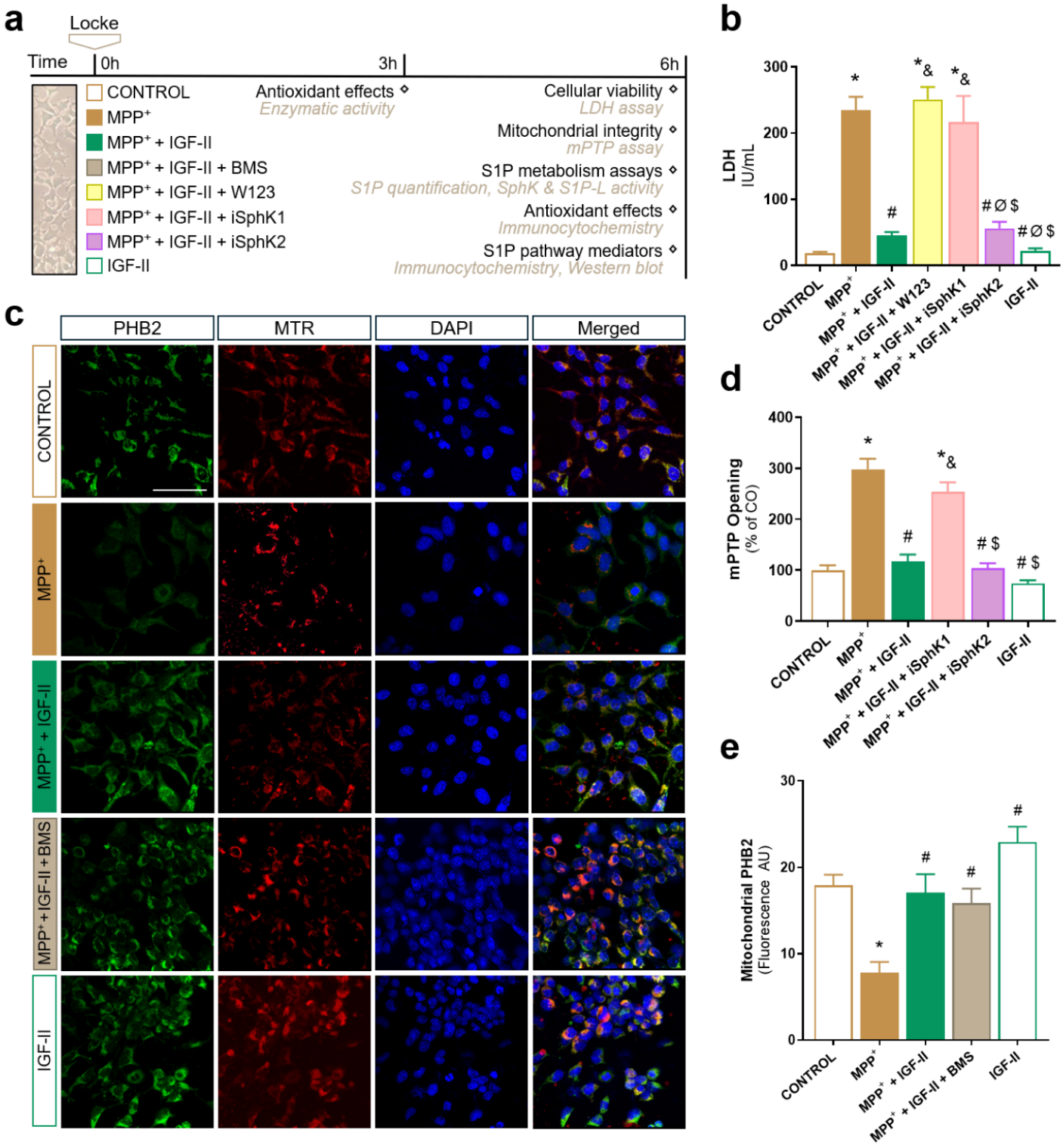


Figure 1

IGF-II protects mitochondrial function and viability from MPP^+-induced damage via SphK1/$S1P_1$-R

a) Experimental timeline and treatment groups in SN4741 dopaminergic cells. Cells were treated with IGF-II alone or in combination with specific inhibitors (BMS: IGF-1R/IR inhibitor; W123: $S1P_1$-R antagonist; iSphK1/iSphK2: isoform-specific sphingosine kinase inhibitors) and challenged with MPP^+ for 3 or 6

hours. **b)** Assessment of cellular death through LDH release. **c)** Representative confocal microscopy images of SN4741 cells showing mitochondrial PHB2 (green), MTR (red), and DAPI nuclear staining (blue). Scale bar = 50 µm. **d)** Quantification of mPTP opening expressed as a percentage of control cells. **e)** Quantitative analysis of PHB2 mitochondrial fluorescence intensity. Data were combined from at least 4 independent experiments and are expressed as mean ± SEM. Statistical significance was determined by one-way ANOVA followed by Tukey's post-hoc test. Symbols indicate $p < 0.05$ for the following comparisons: * vs. CONTROL; # vs. MPP^+; & vs. MPP^+ + IGF-II; Ø vs. MPP^+ + IGF-II + W123; $ vs. MPP^+ + IGF-II + iSphK1; @ vs. MPP^+ + IGF-II + iSphK2.

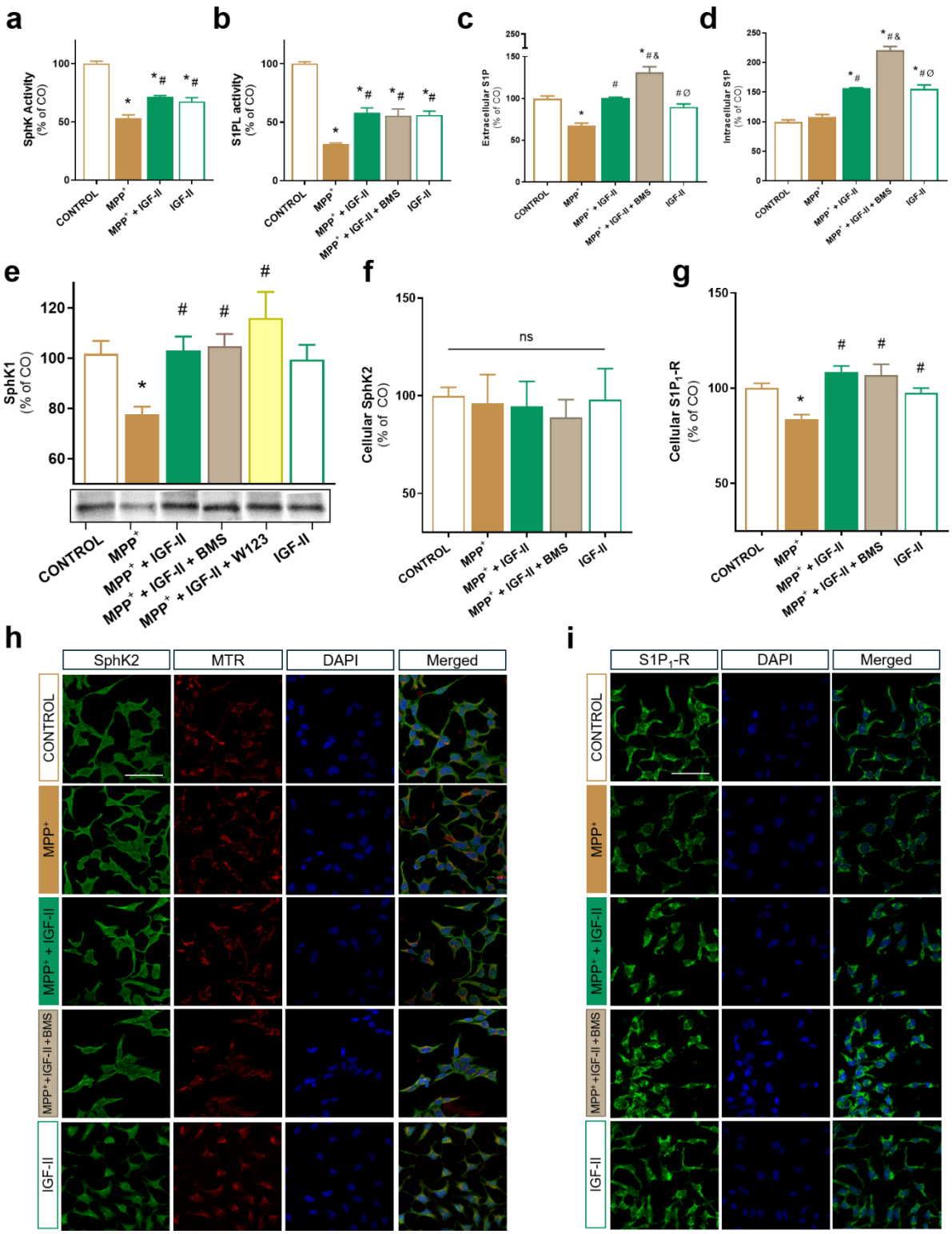


Figure 2

IGF-II orchestrates sphingolipid metabolism and S1P signalling homeostasis to counteract MPP$^+$-induced impairment

a) Global SphK enzymatic activity in SN4741 cells, expressed as a percentage of control cells. **b)** S1PL activity normalised to control cells. **c–d)** Quantitative analysis of **(c)** extracellular and **(d)** intracellular

S1P levels, expressed as a percentage of control cells**. e)** Representative Western Blot and densitometric analysis of SphK1 protein expression. Normalisation was performed using total protein loading (Stain-Free technology) and against control levels. **f)** Quantitative immunofluorescence analysis of SphK2 expression levels. Results are expressed as AU Fluorescence against control levels. **g)** Quantitative immunofluorescence analysis of $S1P_1$-R expression levels. Results are expressed as AU Fluorescence against control levels. **h–i)** Representative confocal microscopy panels for **(h)** SphK2 (green), MTR (red), and DAPI (blue), and **(i)** $S1P_1$-R (green) with DAPI (blue). Scale bar = 50 μm. Data were combined from at least 4 independent experiments and are expressed as mean ± SEM. Statistical significance was determined by one-way ANOVA followed by Tukey's post-hoc test. Symbols indicate $p < 0.05$ for the following comparisons: * vs. CONTROL; # vs. MPP^+; & vs. MPP^+ + IGF-II; Ø vs. MPP^+ + IGF-II + W123; $ vs. MPP^+ + IGF-II + iSphK1; @ vs. MPP^+ + IGF-II + iSphK2. ns denote $p > 0.05$ between conditions.

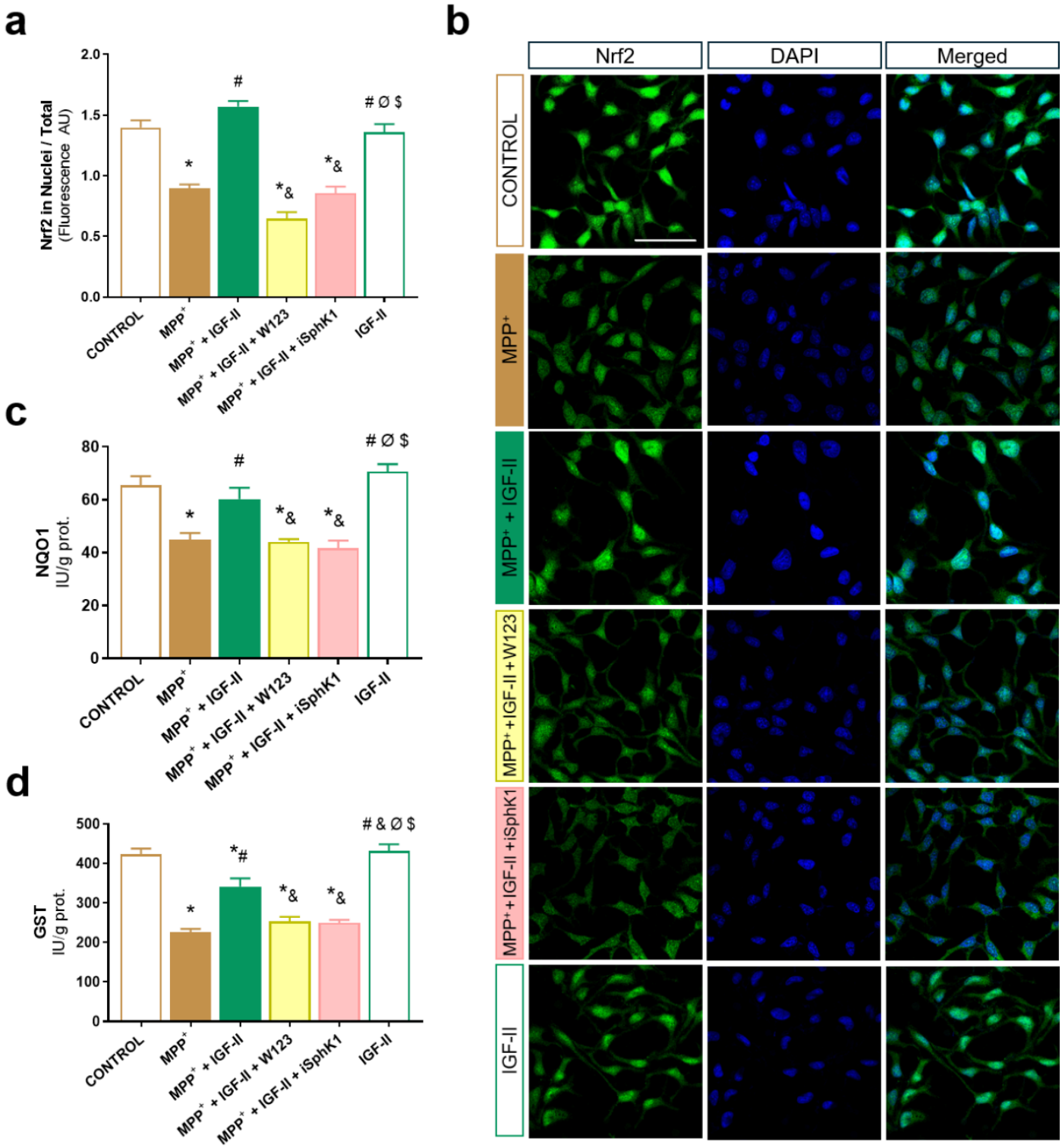


Figure 3

IGF-II/SphK1/S1P$_1$ signalling drives Nrf2 antioxidant activation and nuclear translocation

a) Quantitative immunofluorescence analysis of nuclear Nrf2 translocation, expressed as the ratio of nuclear to total fluorescence intensity. **b)** Representative confocal microscopy images of SN4741 cells showing Nrf2 (green) and DAPI nuclear staining (blue). The merged panels illustrate Nrf2 localisation

within the nucleus. Scale bar = 50 μm. **c–d)** Enzymatic activity of the Nrf2-target Phase II detoxifying enzymes **(c)** NQO1 and **(d)** GST, both data expressed as International Units per gram of protein. Data were combined from at least 4 independent experiments and are expressed as mean ± SEM. Statistical significance was determined by one-way ANOVA followed by Tukey's post-hoc test. Symbols indicate $p < 0.05$ for the following comparisons: * vs. CONTROL; # vs. MPP^+; & vs. MPP^+ + IGF-II; Ø vs. MPP^+ + IGF-II + W123; $ vs. MPP^+ + IGF-II + iSphK1; @ vs. MPP^+ + IGF-II + iSphK2.

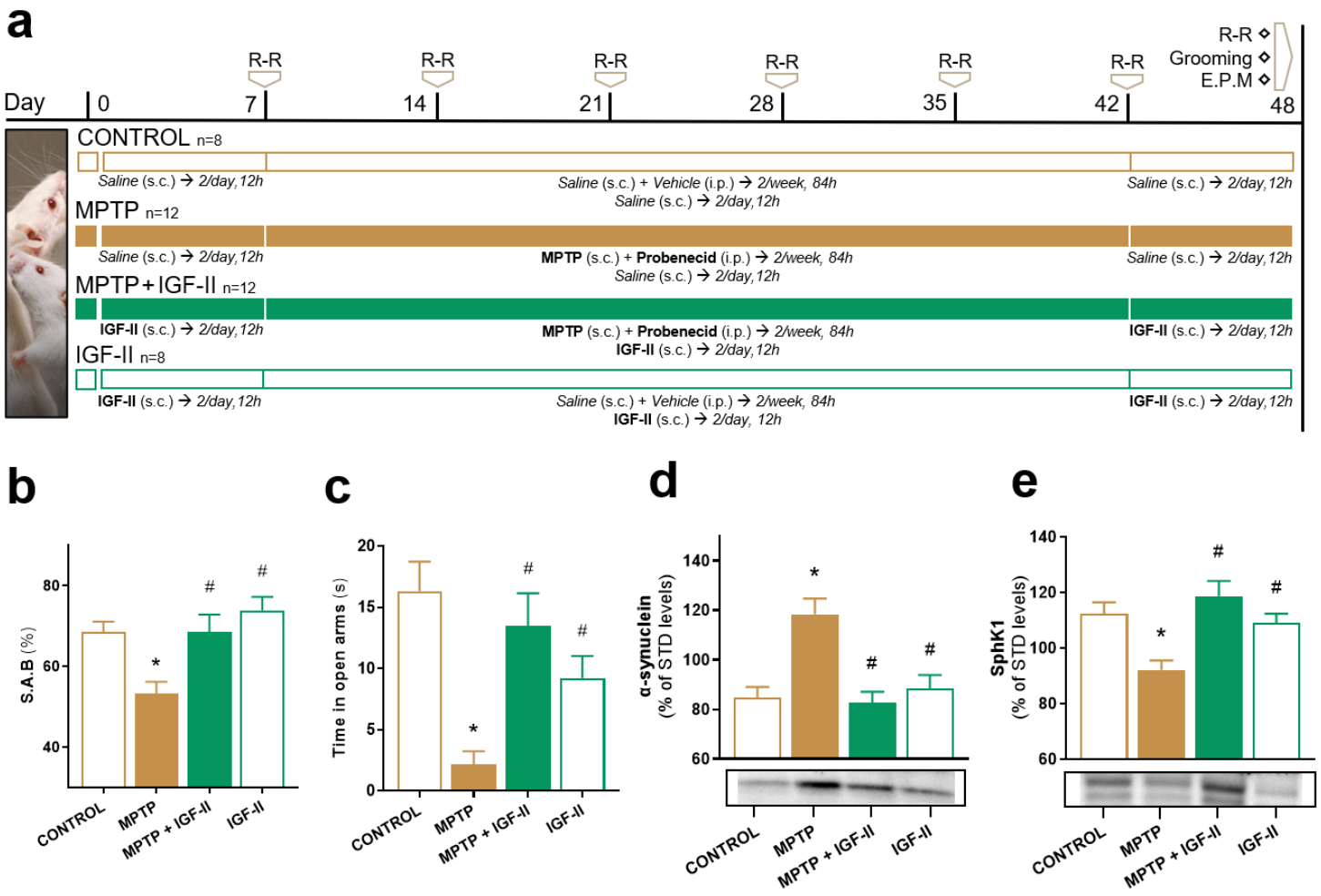


Figure 4

IGF-II preserves motor and non-motor function while reducing α-synuclein pathology in chronic MPTP-treated mice.

a) Experimental design for the chronic in vivo model. C57BL/6 mice were divided into four groups (Control, MPTP, MPTP + IGF-II, and IGF-II alone). The chronic MPTP/p regimen was administered for 5 weeks, with IGF-II (or vehicle) provided throughout the experimental period. Behavioural assessments were conducted during (Rota-Rod) and at the end of the treatment (Y-maze and EPM) before histological and biochemical processing. **b)** Assessment of spatial working memory through S.A.B. % in the Y-maze. **c)** Evaluation of anxiety-like behaviour in the EPM, expressed as time spent in the open arms (s). **d-e)** Representative Western Blot and quantitative analysis of **(d)** α-synuclein and **(e)** SphK1 expression in the

substantia nigra. Pooled tissue samples were generated from 3–4 randomly assigned mice from the same experimental group. Values are expressed as a percentage of a standardised protein pool (STD), obtained from the *substantia nigra* of four untreated, age-matched mice, which was loaded onto every gel to ensure accurate inter-blot normalisation. Data were combined from at least 4 independent experiments and are expressed as mean ± SEM. Statistical analysis was performed using one-way ANOVA followed by Tukey's post-hoc test. Symbols indicate $p<0.05$ for the following comparisons: * vs CONTROL; # vs MPP^+.

Supplementary Files

This is a list of supplementary files associated with this preprint. Click to download.

- Supplementarymaterial.pdf
- BlotsGelsPAPER.pdf